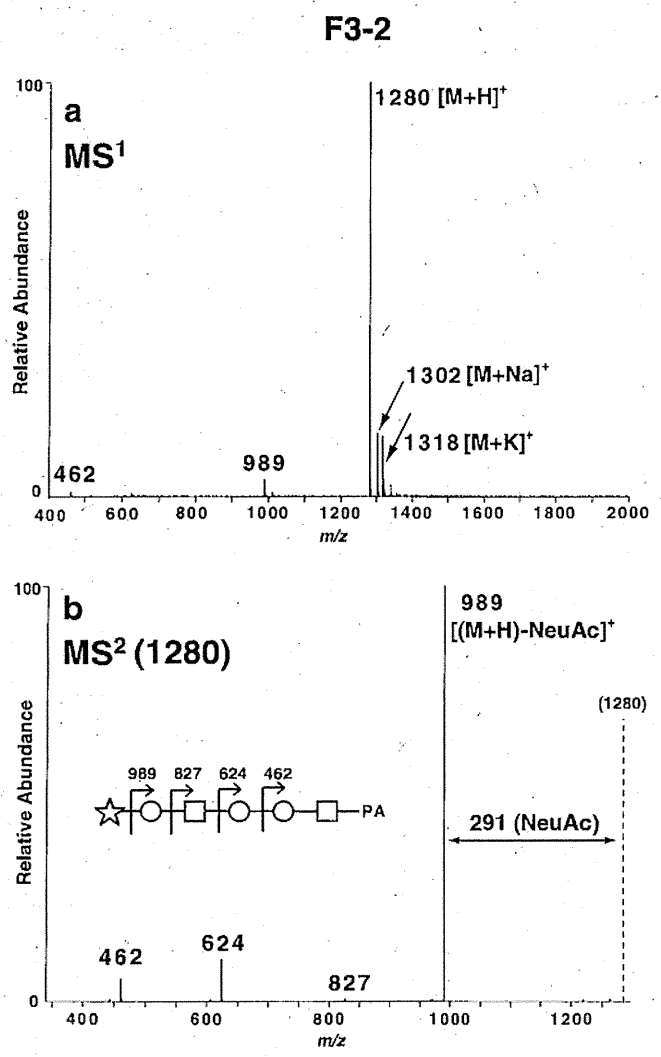

Fig. 3 $MS^{1,2}$ spectra of F3-2. a MS^1 spectra of F3-2; b MS^2 spectra of $[M+H]^+$ precursor ion at *m/z* 1280 detected in MS^1 of A. The MS/MS fragment ions were assigned as shown schematically. Symbol representations of glycans are as follows: Hex, open circle; HexNAc, open square; Neu5Ac, open star

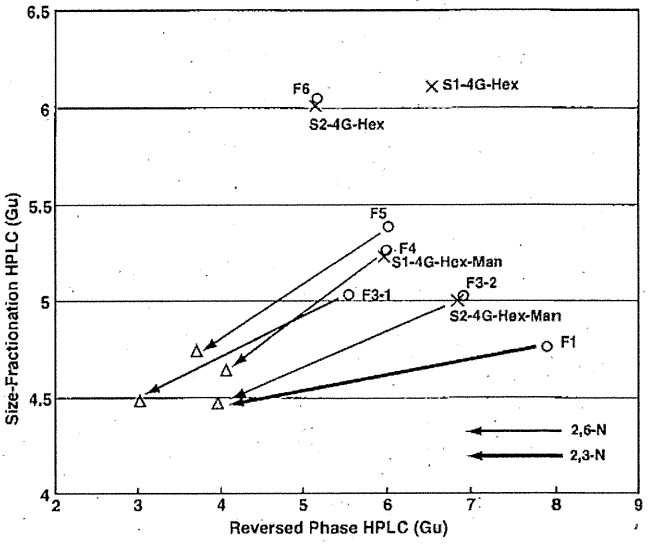

Fig. 4 Digestion of PA-oligosaccharides with sialidase. The elution profiles of PA-*N*-glycans are summarized in the form of a 2-D map. Xs indicate the positions of the authentic PA-*N*-glycans (Table 1). Open circles indicate the positions of free Neu5Ac-containing *N*-glycans, F1, F3-1, F3-2, F4, F5 and F6. Triangles indicate the positions of the digested products with sialidase. Thin lines indicate the direction of the change after α2,3-sialidase digestions of F3-1, F3-2, F4 and F5 under the conditions where the enzyme digests Neu5Ac in both α2-3- and α2-6-linkages (abbreviated as 2,6-N). Thick lines indicate the direction of the change after α2,3-sialidase digestions of F1 under the conditions where the enzyme specifically digests α2-3-linked Neu5Ac (abbreviated as 2,3-N)

likely to be digestion products of a disialylated complex biantennary *N*-glycan; specifically, cleavage of the *N,N'*-diacetylchitobiose core linkage (GlcNAcβ1-4GlcNAc) and removal of either the Manα1-3 or Manα1-6 arm from the biantennary form (Fig. 1). Hence, the authentic free complex-type *N*-glycans were synthesized from SGP (Fig. 1, see Material and Methods). F4 and F3-2 coincided with the position of the standard S1-4G-Hex-Man and S2-4G-Hex-Man, respectively, on the 2-D map (Fig. 4). These results were also confirmed by MS analyses. Thus, free oligosaccharides F4 and F3-2 were estimated to be Neu5Acα2-6Galβ1-4GlcNAcβ1-2Manα1-6Manβ1-4GlcNAc and Neu5Acα2-6Galβ1-4GlcNAcβ1-2Manα1-3Manβ1-4GlcNAc, respectively (Table 3). The structures of the other two kinds of free α2,6-Neu5Ac-linked oligosaccharides, F3-1 and F5, were thought to be either Neu5Acα2-6Galβ1-4GlcNAcβ1-6Manα1-6Manβ1-4GlcNAc or Neu5Acα2-6Galβ1-4GlcNAcβ1-4Manα1-3Manβ1-4GlcNAc, based on the branching pattern of typical tetraantennary *N*-glycans. However, we were unable to unambiguously confirm this structure. Hence, the structures of F3-1 and F5 were indicated to be Neu5Acα2-6Galβ1-4GlcNAcβ-Manα-Manβ1-4GlcNAc, without the linkage position of the fourth GlcNAc and third Man residues from the reducing terminus (Table 3). Neu5Ac is linked to F1 *via* α2-3 linkage. The desialylated product of F1 is identical to desialylated F3-2, indicating that the structure of F1 is Neu5Acα2-3Galβ1-4GlcNAcβ1-2Manα1-3Manβ1-4GlcNAc (Table 3, Fig. 4).

Group 2 and Group 3

On the 2D map, F6 coincided with the position of S2-4G-Hex, but not with S1-4G-Hex (Figs. 1 and 4). The structure of F6 was predicted to be Neu5Acα2-6Galβ1-4GlcNAcβ1-2Manα1-3(Manα1-6)Manβ1-4GlcNAc (Table 3). MS analysis revealed the compositional sequence of F2 (Group 3 glycan) to be Neu5Ac-HexNAc-HexNAc-Hex-Hex-HexNAc (data not shown). Neu5Ac was linked *via* α2-6 to the non-reducing terminus. Previous reports showed the presence of a (sialyl) LacdiNAc structure (GalNAcβ1-

4GlcNAc) [19], so we reasoned that F2 is Neu5Acα2-6GalNAc-GlcNAcβ-Manα-Manβ1-4GlcNAc. However, the subterminal residue could not be confirmed as GalNAc in this study, F2 is indicated to be Neu5Acα2-6HexNAc-GlcNAcβ-Manα-Manβ1-4GlcNAc (Table 3).

The structure of GSLs and free oligosaccharides of colorectal cancers

The profiling of acidic GSLs and free oligosaccharides of colorectal cancer cells and normal colorectal epithelial cells from representative cases are shown in Fig. 2a and b, respectively. Two major peaks, G1 (GM3) and G2 (LST-c), were obtained in acidic GSLs of colorectal cancer cells (Fig. 2a). The free oligosaccharide, corresponding to F3-2, was observed as a very minor peak, which is much lower than the GSLs, G1 (GM3) and G2 (LST-c). In the profiling of normal epithelial cells, free oligosaccharides could not be detected (Fig. 2b).

Accumulation of large amounts of free Neu5Ac-containing complex-type N-glycans in pancreatic cancer cells

The structures of GSLs and free oligosaccharides of pancreatic cancer cells and their normal pancreatic cells from five patients have been analyzed. Free oligosaccharides were obtained as major components in the pancreatic cancer cells from three out of the five cases (cases 1, 2 and 3, Supplementary Table 1). Pancreatic cancer cells derived from the two other cases contained free oligosaccharides as very minor components (cases 4 and 5, Supplementary Table 1). However, these free oligosaccharides were undetectable in normal pancreatic cells from all five cases. Furthermore, the amount of the major free *N*-glycans of pancreatic cancer cells was much higher than those of colorectal cancers cells. The profile of oligosaccharides from pancreatic cancer cells (Fig. 2c, e, g) and the corresponding normal pancreatic epithelial cells (Fig. 2d, f, h) from three cases, all of which showed an accumulation of free oligosaccharides as major components in the pancreatic cancer cells, are shown in Fig. 2c–h.

Figure 2c shows the profile of PA-glycans of case 1 (Supplementary Table 1) i.e., where free *N*-glycans were most abundantly accumulated in pancreatic cancer cells among the five cases. The corresponding profile for normal pancreatic cells from the same case is shown in Fig. 2d. In the GSLs, G1 (GM3) was expressed as the dominant component in both pancreatic cancer cells and normal pancreatic cells, and the expression levels of GM3 of these cells were much higher than those of colorectal cancer cells and normal colorectal cells (Figure 2a–d). In addition to GSLs (G1, G3 and G4), a variety of free oligosaccharides were also detected in cancer cells, but not normal cells. The abundance of the free *N*-glycans exceeded about 2-fold that of GSLs (Fig. 2c, d). Six peaks, F1, F2, F3, F4, F5 and F6, corresponding to free *N*-glycans, were observed. Reversed phase HPLC of each peak revealed that they were composed of 7 oligosaccharides, F1, F2, F3-1, F3-2, F4, F5 and F6. The abundance of each *N*-glycan is summarized in Table 3. All but 1 (F1) of the 7 glycans were α2-6-Neu5Ac-linked *N*-glycans, which represented more than 95 % of the total amount of free *N*-glycans in these samples (Table 3). F3-2 was most abundant, and the amount of other 6 glycans was much lower than that of F3-2. Among the four kinds of α2-6-sialylated oligosaccharides in group 1, the relative amount of each species was as follows: F3-2 (72 %) >>F4 (10 %)>F3-1 (6 %)>F5 (1 %) (numbers in parentheses indicate the percentage of each glycan relative to total free *N*-glycan). It is noteworthy that this order is common to all the cases of pancreatic cancers.

The profiling of GSLs and free *N*-glycans of pancreatic cancer and normal pancreatic cells from the other two cases are shown in Fig. 2e and f (case 2, Supplementary Table 1) and in Fig. 2g and h (case 3, Supplementary Table 1). The profiles are similar to that of case 1 described above, although the amounts of free *N*-glycans were considerably lower for cases 2 and 3. Nonetheless, the amount of free *N*-glycans was still comparable to that of GSLs (Fig. 2c, e, g). Akin to the previous case, the relative amount of group 1 oligosaccharides was as follows: F3-2 >>F4>F3-1>F5 (Table 3).

Discussion

Structural analyses of oligosaccharides associated with pancreatic cancers revealed, unlike colorectal cancer cells, the presence of a variety of free Neu5Ac-containing complex-type *N*-glycans. The relative amounts of these free Neu5Ac-containing complex-type *N*-glycans were comparable to or much higher than those of GSLs in most, but not all, pancreatic cancers. High levels of free Neu5Ac-containing N-glycans were observed in the pancreatic cancer cells from three out of the five cases, but correlation between clinicopathological features and the amounts of free oligosaccharides were not found.

The free *N*-glycans accumulated in cancer cells derived from the three human pancreatic cancer cases described in this study (cases 1, 2 and 3) and the previously studied colorectal cancer cases [8–11] were found to possess several common characteristic features. Specifically, (i) almost all (>95 %) of the free *N*-glycans were composed of α2-6-Neu5Ac-linked glycans, with α2-3-sialylated glycans making up a very minor part, and (ii) the proportion of each free *N*-glycan relative to total free glycans was to some extent dependent on its pentasaccharide backbone. Namely, free α2-6-

Neu5Ac-linked *N*-glycans having a Galβ1-4GlcNAcβ1-2Manα1-3Manβ1-4GlcNAc backbone were the most abundant species (i.e., 48–72 % of total free *N*-glycan content). The second most abundant glycans had a Galβ1-4GlcNAcβ1-2Manα1-6Manβ1-4GlcNAc backbone (8–24 %), followed by glycans with either a Galβ1-4GlcNAcβ1-6Manα1-6Manβ1-4GlcNAc or Galβ1-4GlcNAcβ1-4Manα1-3Manβ1-4GlcNAc backbone. These results indicated that the branch on the α6-Man arm of biantennary *N*-glycans was preferentially removed. Thus, F3-2 (Neu5Acα2-6Galβ1-4GlcNAcβ1-2Manα1-3Manβ1-4GlcNAc) was most abundant among the free Neu5Ac-containing *N*-glycans in the cancers examined.

The occurrence of free complex-type *N*-glycans in mammals has been reported in mouse liver and in human stomach cancer derived cell lines, MKN7 and MKN45 cells [12, 16]. In mouse liver, only free complex-type biantennary, but not monoantennary, *N*-glycans were observed. This observation differs from the findings reported in this study. Free monoantennary *N*-glycan was found in MKN7 and MKN45 cells. Similar to our findings, F3-2 (Neu5Acα2-6Galβ1-4GlcNAcβ1-2Manα1-3Manβ1-4GlcNAc) was most abundant in MKN7 and MKN45 cells. Furthermore, the amounts of F3-2 in MKN7 and MKN45 were about 600 and 380 pmol/10^6 cells, respectively [12]. However, significant differences in the composition of accumulated free oligosaccharides were found between the two kinds of cell lines and human pancreatic cancers. Almost all the free *N*-glycans in human cancers examined in this study were composed of monosialylated hexasaccharide with a singly trimmed core structure (group 1, and 3) along with F6 (group 2), possessing an intact trimannosyl core structure (Table 3). By contrast, in MKN7 and MKN45 cells, F3-2 was the only monosialylated hexasaccharide with a singly trimmed core structure among the various free *N*-glycans, and F6 as the major component. Furthermore, free multiply sialylated *N*-glycans, which could not be detected in human cancers, were abundantly present in MKN7 and MKN45 cells.

In the same report of MKN7 and MKN45 cells, a mechanism responsible for the accumulation of free Neu5Ac-containing *N*-glycans was suggested based on biochemical analyses to be due to insufficient lysosomal function, inefficient degradation of the free *N*-glycans in the lysosomes, as well as the leakage of lysosomal components including free *N*-glycans into the cytosol [12]. This hypothesis is further supported by the findings that F3-2, F1 and F6 are contained in excessive urinary excretion from patients with the lysosomal disease, sialidosis [20]. A similar mechanism might be responsible for the accumulation of free complex-type *N*-glycans in human pancreatic cancer cells, though experimental evidence needs to be provided by further studies.

In this study, we focused on the analysis of the structures of GSLs and free glycans. The other kinds of glycoconjugates, such as *N*-linked glycans attached as glycoproteins, are also very interesting and important targets to investigate the difference between pancreatic and normal pancreatic cells.

In summary, we have unequivocally demonstrated that substantial amounts of free Neu5Ac-complex-type *N*-glycans accumulate in human pancreatic cancers. By contrast, in most normal epithelial cells these glycan species were undetectable. It is possible that these glycans might be developed as novel tumor markers for cancers. However, further validation studies will be needed prior to clinical application of these candidate markers.

Acknowledgements This work was supported in part by the Program for Promotion of Fundamental Studies in Health Sciences of the National Institute of Biomedical Innovation (NIBIO). This study was performed in part as a research program of the Project for Development of Innovative Research on Cancer Therapeutics (P-Direct), Ministry of Education, Culture, Sports, Science and Technology of Japan.

References

1. Hakomori, S.: Glycosylation defining cancer malignancy: new wine in an old bottle. Proc. Natl. Acad. Sci. U.S.A. **99**(16), 10231–10233 (2002)
2. Lau, K.S., Dennis, J.W.: N-Glycans in cancer progression. Glycobiology **18**(10), 750–760 (2008)
3. Brockhausen, I.: Pathways of O-glycan biosynthesis in cancer cells. Biochim. Biophys. Acta **1473**(1), 67–95 (1999)
4. Kim, Y.J., Varki, A.: Perspectives on the significance of altered glycosylation of glycoproteins in cancer. Glycoconj. J. **14**(5), 569–576 (1997)
5. Saldova, R., Wormald, M.R., Dwek, R.A., Rudd, P.M.: Glycosylation changes on serum glycoproteins in ovarian cancer may contribute to disease pathogenesis. Dis. Markers **25**(4–5), 219–232 (2008)
6. Kannagi, R., Izawa, M., Koike, T., Miyazaki, K., Kimura, N.: Carbohydrate-mediated cell adhesion in cancer metastasis and angiogenesis. Cancer Sci. **95**(5), 377–384 (2004)
7. Peracaula, R., Barrabes, S., Sarrats, A., Rudd, P.M., de Llorens, R.: Altered glycosylation in tumours focused to cancer diagnosis. Dis. Markers **25**(4–5), 207–218 (2008)
8. Shida, K., Misonou, Y., Korekane, H., Seki, Y., Noura, S., Ohue, M., Honke, K., Miyamoto, Y.: Unusual accumulation of sulfated glycosphingolipids in colon cancer cells. Glycobiology **19**(9), 1018–1033 (2009)
9. Korekane, H., Tsuji, S., Noura, S., Ohue, M., Sasaki, Y., Imaoka, S., Miyamoto, Y.: Novel fucogangliosides found in human colon adenocarcinoma tissues by means of glycomic analysis. Anal. Biochem. **364**(1), 37–50 (2007)
10. Shida, K., Korekane, H., Misonou, Y., Noura, S., Ohue, M., Takahashi, H., Ohigashi, H., Ishikawa, O., Miyamoto, Y.: Novel ganglioside found in adenocarcinoma cells of Lewis-negative patients. Glycobiology **20**(12), 1594–1606 (2010)
11. Misonou, Y., Shida, K., Korekane, H., Seki, Y., Noura, S., Ohue, M., Miyamoto, Y.: Comprehensive clinico-glycomic study of 16 colorectal cancer specimens: elucidation of aberrant glycosylation and its mechanistic causes in colorectal cancer cells. J. Proteome Res. **8**(6), 2990–3005 (2009)
12. Ishizuka, A., Hashimto, Y., Naka, R., Kinoshita, M., Kakehi, K., Seino, J., Funakoshi, Y., Suzuki, T., Kameyama, A., Narimatsu, H.: Accumulation of free complex-type N-glycans in MKN7 and MKN45 stomach cancer cells. Biochem. J. **413**(2), 227–237 (2008)

13. Moore, S.E.: Oligosaccharide transport: pumping waste from the ER into lysosomes. Trends Cell Biol. **9**(11), 441–446 (1999)
14. Suzuki, T., Funakoshi, Y.: Free N-linked oligosaccharide chains: formation and degradation. Glycoconj. J. **23**(5–6), 291–302 (2006)
15. Winchester, B.: Lysosomal metabolism of glycoproteins. Glycobiology **15**(6), 1R–15R (2005)
16. Ohashi, S., Iwai, K., Mega, T., Hase, S.: Quantitation and isomeric structure analysis of free oligosaccharides present in the cytosol fraction of mouse liver: detection of a free disialobiantennary oligosaccharide and glucosylated oligomannosides. J. Biochem. **126**(5), 852–858 (1999)
17. Natsuka, S., Hase, S.: Analysis of N- and O-glycans by pyridylamination. Methods Mol. Biol. **76**, 101–113 (1998)
18. Chen, Y.J., Wing, D.R., Guile, G.R., Dwek, R.A., Harvey, D.J., Zamze, S.: Neutral N-glycans in adult rat brain tissue–complete characterisation reveals fucosylated hybrid and complex structures. Eur. J. Biochem. **251**(3), 691–703 (1998)
19. Dell, A., Morris, H.R., Easton, R.L., Panico, M., Patankar, M., Oehniger, S., Koistinen, R., Koistinen, H., Seppala, M., Clark, G.F.: Structural analysis of the oligosaccharides derived from glycodelin, a human glycoprotein with potent immunosuppressive and contraceptive activities. J. Biol. Chem. **270**(41), 24116–24126 (1995)
20. Strecker, G., Peers, M.C., Michalski, J.C., Hondi-Assah, T., Fournet, B., Spik, G., Montreuil, J., Farriaux, J.P., Maroteaux, P., Durand, P.: Structure of nine sialyl-oligosaccharides accumulated in urine of eleven patients with three different types of sialidosis. Mucolipidosis II and two new types of mucolipidosis. Eur. J. Biochem. **75**(2), 391–403 (1977)

Glycobiology vol. 23 no. 6 pp. 634–642, 2013
doi:10.1093/glycob/cws132
Advance Access publication on September 12, 2012

Occurrence of free deaminoneuraminic acid (KDN)-containing complex-type *N*-glycans in human prostate cancers

Masahiko Yabu[2], Hiroaki Korekane[3], Koji Hatano[4], Yasufumi Kaneda[5], Norio Nonomura[4], Chihiro Sato[6], Ken Kitajima[6], and Yasuhide Miyamoto[1,2]

[2]Department of Immunology, Osaka Medical Center for Cancer and Cardiovascular Diseases, 1-3-3 Nakamichi, Higashinari-ku, Osaka 537-8511, Japan; [3]Systems Glycobiology Research Group, Chemical Biology Department, RIKEN Advanced Science Institute, 2-1 Hirosawa, Wako, Saitama 351-0198, Japan; [4]Department of Urology and; [5]Department of Gene Therapy Science, Graduate School of Medicine, Osaka University, 2-2 Yamadaoka, Suita, Osaka 565-0871, Japan; and [6]Bioscience and Biotechnology Center, Nagoya University, Nagoya 464-8601, Japan

Received on August 16, 2012; revised on September 5, 2012; accepted on September 6, 2012

We previously reported on the accumulation of a substantial amount of free *N*-acetylneuraminic acid (Neu5Ac)-containing complex-type *N*-glycans in human pancreatic cancer cells (Yabu M, Korekane H, Takahashi H, Ohigashi H, Ishikawa O, Miyamoto Y. 2013. Accumulation of free Neu5Ac-containing complex-type *N*-glycans in human pancreatic cancers. *Glycoconj J*, 30(3):247-256). In the present paper, we further extend our cancer glycomic study of human prostate cancer. Specifically, we demonstrate that, in addition to the free Neu5Ac-containing *N*-glycans, significant amounts of free deaminoneuraminic acid (KDN, 2-keto-3-deoxy-D-*glycero*-D-*galacto*-nononic acid)-containing *N*-glycans had accumulated in the prostate cancer tissues from four of five patients. Indeed, in one of the four cases, the free KDN glycans accumulated as major components in prostate cancer tissue. The structures of the KDN-containing free oligosaccharides were analyzed by a variety of methods. Specifically, we used fluorescent labeling with aminopyridine combined with two-dimensional mapping, KDNase digestion and mass spectrometry to facilitate identification. The analysis also utilized newly synthesized KDN-linked oligosaccharides as standards. The prostate-specific glycans were composed of five species having the following sequence, KDN-Gal-GlcNAc-Man-Man-GlcNAc (α2,6-KDN-linked glycans being the dominant form). The most abundant free KDN-containing *N*-glycan was KDNα2-6Galβ1-4GlcNAcβ1-2Manα1-3Manβ1-4GlcNAc followed by KDNα2-6Galβ1-4GlcNAcβ1-2Manα1-6Manβ1-4GlcNAc. This is the first study to show unequivocal chemical evidence for the occurrence of KDN glycoconjugates in human tissues together with their detailed structures. These oligosaccharides might be developed as tumor markers, especially for prostate cancer.

Keywords: free oligosaccharide / KDN / *N*-glycans / prostate cancer

Introduction

Remarkable alterations in oligosaccharide structures are associated with many human diseases, including cancers (Kim and Varki 1997; Brockhausen 1999; Hakomori 2002; Lau and Dennis 2008). Numerous clinicopathological and biochemical studies have suggested the involvement of aberrant glycosylation in cancer malignancy, such as metastasis and invasion (Kannagi et al. 2004). Furthermore, altered carbohydrate determinants, including tumor-associated carbohydrate antigens such as SLe^a and SLe^x have been utilized as useful tumor markers for the diagnosis of cancer (Peracaula et al. 2008; Saldova et al. 2008). Thus, cancer glycomic analyses have been widely used as a valuable tool to investigate the involvement of glycosylation in cancer malignancy as well as to find novel tumor marker candidates (Narimatsu et al. 2010; Alley et al. 2012). We also have conducted accurate structural analysis of glycosphingolipids (GSLs) derived from colorectal cancers of more than 60 patients in our laboratory (Misonou et al. 2009; Shida et al. 2009). Our investigations identified alterations in the structures of GSLs related to cancers and established that these characteristic changes tend to be associated with specific clinical features such as hepatic metastasis. Moreover, sulfated GSLs were found to abnormally accumulate in colon cancers that were predicted to have low metastatic potential. We identified two kinds of novel tumor-associated carbohydrate antigens, Neu5Acα2-6(Fucα1-2)Galβ1-4GlcNAcβ1-3Galβ1-4Glc (α2,6-sialylated type 2H) and Neu5Acα2-6(Fucα1-2)Galβ1-3GlcNAcβ1-3Galβ1-4Glc (α2,6-sialylated type 1H), both of which are isomers of SLe^a and SLe^x (Korekane et al. 2007; Shida et al. 2010), and α2,6-sialylated type 1H is specific to Lewis-negative patients. The evaluation of these two carbohydrate antigens as tumor markers is currently underway in our laboratory.

[1]To whom correspondence should be addressed: Tel: +81-6-6972-1181; Fax: +81-6-6973-5691; e-mail: miyamoto-ya@mc.pref.osaka.jp

Furthermore, subsequent glycomic analyses revealed that large amounts of free Neu5Ac (*N*-acetylneuraminic acid)-containing complex-type *N*-glycans, almost all of which were the α2,6-Neu5Ac-linked form (with Neu5Acα2-6Galβ1-4GlcNAcβ1-2Manα1-3Manβ1-4GlcNAc being the most abundant), were found to accumulate in pancreatic cancer tissue. However, the levels of free *N*-glycans in colorectal cancer cells and in normal colorectal and pancreatic tissues were barely detectable (Yabu et al. 2013).

In the present study, we have extensively analyzed the structures of oligosaccharides in GSLs and free oligosaccharides derived from prostate cancers. These analyses revealed that, in addition to the free Neu5Ac-containing *N*-glycans accumulated in pancreatic cancer, a relatively large amount of free deaminoneuraminic acid (KDN, 2-keto-3-deoxy-D-*glycero*-D-*galacto*-nononic acid)-containing *N*-glycans were also found to accumulate in prostate cancers. With regard to KDN, refer to the review article by Inoue and Kitajima (2006). KDN is an unusual type of sialic acid that was first discovered in the cortical alveolar polysialoglycoprotein of rainbow trout eggs (Nadano et al. 1986). Subsequent studies revealed that KDN, like the typical type sialic acid Neu5Ac, occurs widely among vertebrates and bacteria, although KDN is only abundant in lower vertebrates and pathogenic bacteria. In mammals, Neu5Ac occurs abundantly in both normal and tumor tissues, whereas KDN is almost undetectable (Inoue et al. 1996). Until now, there have been few studies to show the unequivocal occurrence of KDN-containing glycoconjugates in human tissues or their precise structures. In this paper, the detailed structures of these free Neu5Ac- and KDN-containing complex-type *N*-glycans that accumulate in human prostate cancers are presented.

Results

Preparation of pyridylaminated oligosaccharides from human prostate cancers

We analyzed the structures of GSLs and free oligosaccharides of prostate cancer tissues derived from five patients (including a primary lesion and a bone metastatic lesion from the same patient). The clinicopathological features of the five prostate cancer patients are described in Supplementary data, Table S1. It is well known that both free oligosaccharides and GSLs, but not glycoproteins, are recovered in lipid fractions from biological samples (Ishizuka et al. 2008). In this study, both free oligosaccharides and GSLs were extracted from the tissues using organic solvent, chloroform/methanol. The oligosaccharide portions of GSLs were released by endoglycoceramidase II, and the reducing ends of the released oligosaccharides of GSLs and free oligosaccharides were tagged with the fluorophore, 2-aminopyridine (2-AP; *Materials and methods*). Authentic pyridylaminated (PA)-oligosaccharides required for the analysis of GSLs and free *N*-glycans are listed in Table I.

Major acidic free oligosaccharides accumulated in human prostate cancers

The structures of neutral oligosaccharides derived from prostate cancers are not shown because these molecules did not display any interesting disease-related changes.

The acidic PA-oligosaccharides from prostate cancer tissues were analyzed by size-fractionation high-performance liquid chromatography (HPLC) (Figure 1A–E). Each of the peaks separated by the size-fractionation HPLC was further separated by reverse-phase HPLC. Additionally, the separated PA-oligosaccharides were subjected to liquid chromatography/electrospray ionization MS/MS (LC/ESI MS^2) analysis. Some of the PA-oligosaccharides were also analyzed after digestion with glycosidase to help ascertain their structures. By means of these combinational analyses, the structures of all the major GSLs could be estimated and the occurrence of a large amount of free sialylated complex-type *N*-glycans in prostate cancers was unequivocally demonstrated. In total, 12 distinct sialylated free oligosaccharides (F1, F2, F3-1, F3-2, F4, F5-1, F5-2, F5-3, F5-4, F6, F7 and F8) were detected as major components in human prostate cancers (Figure 1, Tables II and III). All these glycans were easily predicted to be sialylated free complex-type *N*-glycans having a single HexNAc (probably GlcNAc) at their reducing termini (Gn1 glycans) by mass analyses. Elution positions, mass data and estimated composition of the oligosaccharides are presented in Table II. Based on the composition of monosaccharides, we were able to classify the 12 free *N*-glycans into four groups as follows; group 1 (F3-1, F3-2, F4, F5-1 and F1), group 2 (F5-2, F5-3, F5-4, F6 and F7), group 3 (F8) and group 4 (F2) (Tables II and III). In the following *Results* sections, the structures of these PA-oligosaccharides are described in detail.

Structural analyses of free sialylated complex-type N-glycans

Groups 1, 3 and 4. Glycans of group 1 (F3-1, F3-2, F4, F5-1 and F1), group 3 (F8), and group 4 (F2) were free Neu5Ac-containing complex-type *N*-glycans (Table II). All of these free glycans have been detected in human pancreatic cancer cells (Yabu et al. 2013). Hence, the structures of most of these free glycans were estimated in the previous study and are listed in Table I as standard PA-oligosaccharides. From comparison of the positions on the map to the positions of standard PA-oligosaccharides, F1, F3-2, F4 and F8 are predicted to be Neu5Acα2-3Galβ1-4GlcNAcβ1-2Manα1-3Manβ1-4GlcNAc (N3M3), Neu5Acα2-6Galβ1-4GlcNAcβ1-2Manα1-3Manβ1-4GlcNAc (N6M3), Neu5Acα2-6Galβ1-4GlcNAcβ1-2Manα1-6Manβ1-4GlcNAc (N6M6) and Neu5Acα2-6Galβ1-4GlcNAcβ1-2Manα1-3(Manα1-6)Manβ1-4GlcNAc (N6M3(M6)), respectively (Figure 2). The structures of these two-dimensional (2D) matched oligosaccharides were also confirmed by mass spectrometry. The structures of the remaining three free glycans, F3-1, F5-1 and F2, were unable to be unambiguously determined. F3-1 and F5-1 were thought to be either Neu5Acα2-6Galβ1-4GlcNAcβ1-6Manα1-6Manβ1-4GlcNAc or Neu5Acα2-6Galβ1-4GlcNAcβ1-4Manα1-3Manβ1-4GlcNAc. However, we were unable to unambiguously confirm this structure. Hence, the structures of F3-1 and F5-1 are given as Neu5Acα2-6Galβ1-4GlcNAcβ-Manα-Manβ1-4GlcNAc, without the linkage position of the fourth GlcNAc and third Man residues from the reducing terminus (Table III). F2 was predicted to have a LacdiNAc structure (GalNAcβ1-4GlcNAc) by mass analysis. The structure of F2 was thought to be Neu5Acα2-6GalNAc-GlcNAcβ-Manα-Manβ1-4GlcNAc, although the subterminal residue could not

Table I. Structures and elution positions in HPLC of standard PA-oligosaccharides

Abbreviation	Structure	Elution position in HPLC	
		Size (Gu)	RP (Gu)
GM3 (G1)	Neu5Acα2-3Galβ1-4Glc-PA	2.46	3.00
LST-c (G2)	Neu5Acα2-6Galβ1-4GlcNAcβ1-3Galβ1-4Glc-PA	4.40	3.76
SPG (G3)	Neu5Acα2-3Galβ1-4GlcNAcβ1-3Galβ1-4Glc-PA	4.02	4.52
GD1a (G4)	**Galβ1-3GalNAcβ1-4Galβ1-4Glc-PA** **3 3** **Neu5Acα2 Neu5Acα2**	4.10	5.03
N6M6(M3)	**Neu5Acα2-6Galβ1-4GlcNAcβ1-2Manα1** **6** **Manβ1-4GlcNAc-PA** **3** **Manα1**	6.11	6.55
N6M3(M6) (F8)	**Manα1** **6** **Manβ1-4GlcNAc-PA** **3** **Neu5Acα2-6Galβ1-4GlcNAcβ1-2Manα1**	6.01	5.15
N6M6 (F4)	**Neu5Acα2-6Galβ1-4GlcNAcβ1-2Manα1** **6** **Manβ1-4GlcNAc-PA**	5.21	5.93
N6M3 (F3-2)	**Manβ1-4GlcNAc-PA** **3** **Neu5Acα2-6Galβ1-4GlcNAcβ1-2Manα1**	5.00	6.84
N3M3 (F1)	**Manβ1-4GlcNAc-PA** **3** **Neu5Acα2-3Galβ1-4GlcNAcβ1-2Manα1**	4.76	7.91
K3M6 (F5-4)	**KDNα2-3Galβ1-4GlcNAcβ1-2Manα1** **6** **Manβ1-4GlcNAc-PA**	5.52	5.16
K6M6 (F6)	**KDNα2-6Galβ1-4GlcNAcβ1-2Manα1** **6** **Manβ1-4GlcNAc-PA**	5.78	3.92
K3M3	**Manβ1-4GlcNAc-PA** **3** **KDNα2-3Galβ1-4GlcNAcβ1-2Manα1**	5.30	5.43
K6M3 (F5-3)	**Manβ1-4GlcNAc-PA** **3** **KDNα2-6Galβ1-4GlcNAcβ1-2Manα1**	5.54	4.77

Abbreviations of free *N*-linked glycans: N, M and K represent Neu5Ac, mannose, and KDN, respectively. Numbers mean the linkage position of Neu5Ac (N), third mannose (M) and KDN (K). M3 and M6 given in the parenthesis represent α1-3 and α1-6 mannose branches, respectively. Peak numbers shown in Figure 2 are given in parentheses.

be confirmed as GalNAc. F2 is given as Neu5Acα2-6Hex NAc-GlcNAcβ-Manα-Manβ1-4GlcNAc (Table III).

Group 2. The $MS^{1,2}$ spectra of the five group 2 glycans (F5-2, F5-3, F5-4, F6 and F7) were essentially the same. A representative $MS^{1,2}$ spectrum of F5-3 is shown in Figure 3A and B. The structures of the group 2 free oligosaccharides were judged to be KDN-Gal-GlcNAc-Man-Man-GlcNAc-PA based on α-mannosidase digestion, MS^2 analysis and KDNase digestions (Figure 3A and B). Specifically, (i) these oligosaccharides were completely resistant to α-mannosidase digestion, and thus, the probability of the branched structures, KDN-GlcNAc-Man-(Man-)Man-GlcNAc-PA, could be excluded; (ii) collision-induced dissociation spectra showed that the *m/z* 250 residue, which corresponded to KDN, was linked to the glycans (Figure 3A and B) and (iii) the glycans could not be cleaved by *N*-acetylneuraminidase, but were digested by KDNase, which can digest deaminoneuraminyl but not *N*-acetylneuraminyl linkages. The KDNase digested products of F5-2, F5-3 and F7 co-migrated on the 2D map with the desialylated products of F3-1, F3-2 and F5-1, respectively (Figure 2A and B). Similarly, the KDNase digested products of F5-4 and F6 co-migrated with desialylated F4 on the 2D map (Figure 2A and B). Next, we determined the linkage positions of KDN for the five KDN glycans. First, α2,3- and α2,6-KDN-linked authentic *N*-glycans were enzymatically synthesized from the desialylated F3-1, F3-2, F4 and F5-1 by reaction with cytidine monophospho-KDN (CMP-KDN) catalyzed by α2,3- or α2,6-sialyltransferases. These *N*-glycans were then subjected to 2D mapping and mass analyses (see *Material and methods*, Figure 2C). Our analyses revealed that KDN were linked α2-6 to F5-2, F5-3, F6 and F7 and α2-3 to F5-4 (Figure 2C). Therefore, the structures of F5-2, F5-3, F5-4, F6 and F7 were predicted as listed in Table III. As was the case for F3-1 and F5-1, the structures of F5-2 and F7 were deduced to be KDNα2-6Galβ1-4GlcNAcβ-Manα-Manβ1-4GlcNAc, without the linkage position of the fourth GlcNAc and third Man residues from the reducing terminus.

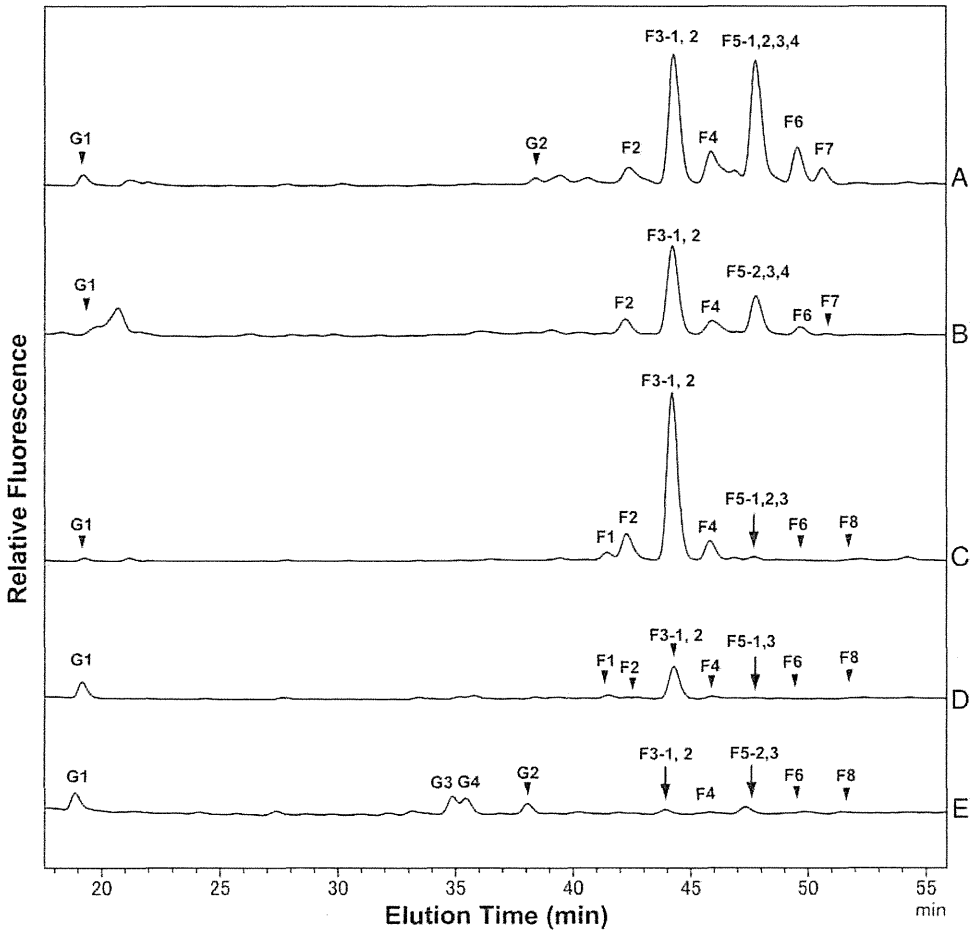

Fig. 1. Size fractionation HPLC of acidic PA-oligosaccharide mixtures obtained from human prostate cancers. (**A–E**) Prostate cancer tissues (100 μg each). (A and B) Bone metastatic lesion and primary lesion from the same patient (case 1, Supplementary data, Table S1); (C–E) Primary lesion from the other three patients (C, case 5; D, case 3; E, case 4; Supplementary data, Table S1). Eight major peaks derived from free *N*-glycans found in prostate cancers are represented as F1–F8 with fraction numbers as per Tables II and III. G1–G4 are the peaks derived from GSLs. The structures of G1–G4 are listed in Table I. The positions of minor peaks that were barely detectable are highlighted by either an arrowhead or an arrow.

Table II. Elution positions in HPLC and mass analysis of sialylated PA-free oligosaccharides obtained from human prostate cancers

Group	Fraction	Elution position in HPLC		Mass (observed)	Mass (calculated)	Estimated composition
		Size (Gu)	RP (Gu)			
1	F3-1	5.04	5.41	1280.5	1280.5 $[M+H]^+$	$NeuAc_1Hex_3HexNAc_2$-PA
	F3-2	5.05	6.78	1280.4	1280.5 $[M+H]^+$	$NeuAc_1Hex_3HexNAc_2$-PA
	F4	5.26	5.93	1280.5	1280.5 $[M+H]^+$	$NeuAc_1Hex_3HexNAc_2$-PA
	F5-1	5.40	5.98	1280.5	1280.5 $[M+H]^+$	$NeuAc_1Hex_3HexNAc_2$-PA
	F1	4.80	7.86	1280.5	1280.5 $[M+H]^+$	$NeuAc_1Hex_3HexNAc_2$-PA
2	F5-2	5.49	3.81	1239.5	1239.5 $[M+H]^+$	$KDN_1Hex_3HexNAc_2$-PA
	F5-3	5.49	4.74	1239.4	1239.5 $[M+H]^+$	$KDN_1Hex_3HexNAc_2$-PA
	F5-4	5.48	5.24	1239.4	1239.5 $[M+H]^+$	$KDN_1Hex_3HexNAc_2$-PA
	F6	5.71	3.90	1239.6	1239.5 $[M+H]^+$	$KDN_1Hex_3HexNAc_2$-PA
	F7	5.86	3.75	1239.5	1239.5 $[M+H]^+$	$KDN_1Hex_3HexNAc_2$-PA
3	F8	6.10	5.16	1442.4	1442.5 $[M+H]^+$	$NeuAc_1Hex_4HexNAc_2$-PA
4	F2	4.83	7.76	1321.5	1321.5 $[M+H]^+$	$NeuAc_1Hex_2HexNAc_3$-PA

Occurrence of both Neu5Ac- and KDN-containing free complex-type N-glycans in prostate cancer

The structures of GSLs and free oligosaccharides from six prostate cancer tissues derived from five patients (including a primary lesion and a bone metastatic lesion from the same patient) have been analyzed. The prominent and striking feature of the profile of prostate cancer was the presence of relatively large amounts of free KDN-containing complex-

Table III. Neu5Ac- and KDN-containing free complex-type *N*-glycans accumulated in human prostate cancers

Group	Fraction	Structure	Amount of glycan (pmol/100 μg protein)				
			(A)	(B)	(C)	(D)	(E)
1	F3-1	Neu5Acα2-6Galβ1-4GlcNAcβ-Manα-Manβ1-4GlcNAc-PA	22.9	5.0	11.2	2.3	1.6
	F3-2	**Manβ1-4GlcNAc-PA** (3) **Neu5Acα2-6Galβ1-4GlcNAcβ1-2Manα1**	60.4	48.7	81.1	15.6	3.2
	F4	**Neu5Acα2-6Galβ1-4GlcNAcβ1-2Manα1** (6) **Manβ1-4GlcNAc-PA**	33.0	11.4	13.0	0.5	0.3
	F5-1	Neu5Acα2-6Galβ1-4GlcNAcβ-Manα-Manβ1-4GlcNAc-PA	3.5	(–)	0.8	0.1	(–)
	F1	**Manβ1-4GlcNAc-PA** (3) **Neu5Acα2-3Galβ1-4GlcNAcβ1-2Manα1**	(–)	(–)	2.1	0.5	(–)
2	F5-2	KDNα2-6Galβ1-4GlcNAcβ-Manα-Manβ1-4GlcNAc-PA	20.8	2.7	0.1	(–)	1.1
	F5-3	**Manβ1-4GlcNAc-PA** (3) **KDNα2-6Galβ1-4GlcNAcβ1-2Manα1**	55.9	19.2	1.4	0.1	4.0
	F5-4	**KDNα2-3Galβ1-4GlcNAcβ1-2Manα1** (6) **Manβ1-4GlcNAc-PA**	5.3	1.1	(–)	(–)	(–)
	F6	**KDNα2-6Galβ1-4GlcNAcβ1-2Manα1** (6) **Manβ1-4GlcNAc-PA**	23.4	5.5	0.2	0.1	0.2
	F7	KDNα2-6Galβ1-4GlcNAcβ-Manα-Manβ1-4GlcNAc-PA	7.7	1.0	(–)	(–)	(–)
3	F8	**Manα1** (6) **Manβ1-4GlcNAc-PA** (3) **Neu5Acα2-6Galβ1-4GlcNAcβ1-2Manα1**	(–)	(–)	0.3	0.1	0.6
4	F2	Neu5Acα2-6HexNAc-GlcNAcβ-Manα-Manβ1-4GlcNAc-PA	6.3	8.3	11.7	0.1	(–)

Estimated structures and the amount of glycans in prostate cancer tissues (cases of Figure 1A–E) are presented. The amount of glycan is expressed as pmol/100 μg protein. (–) indicates that this glycan was not detected in the tissues.

type *N*-glycans. Although prostate cancers from four of the five patients contained the free KDN-containing *N*-glycans, their abundance varied in each patient. Prostate cancers from one case (case 1, Supplementary data, Table S1) contained KDN-linked free oligosaccharides as major components (shown in Figure 1A and B of the metastatic and primary lesion of this case) and prostate cancers from the other three cases (cases 3, 4 and 5, Supplementary data, Table S1) contained KDN-linked free oligosaccharides as minor components (shown in Figure 1C–E).

Figure 1A shows the profiling of GSLs and free oligosaccharides from a bone metastatic lesion of a prostate cancer case (case 1) where a substantial amount of free KDN-containing *N*-glycans had accumulated. Two peaks, G1 (GM3) and G2 LS tetrasaccharide (LST-c), were obtained in acidic GSLs of this case. In addition to these GSLs, a variety of free oligosaccharides were also found as major components in this case. Six peaks, F2, F3, F4, F5, F6 and F7, corresponding to free *N*-glycans were observed. These peaks were much more prominent than those derived from GSLs, G1 (GM3) and G2 (LST-c). Reverse-phase HPLC revealed that peaks F2–F7 were composed of 10 glycans, F2, F3-1, F3-2, F4, F5-1, F5-2, F5-3, F5-4, F6 and F7. Among them, F5-2, F5-3, F5-4, F6 and F7 were classified as group 2 glycans, i.e. free KDN-containing *N*-glycans (Tables II and III). The amount of each glycan is listed in Table III. We reported that almost all of the free *N*-glycans in human pancreatic cancers were composed of α2,6-Neu5Ac-linked glycans, with α2,3-sialylated glycans as minor species (Yabu et al. 2013). As was the case of pancreatic cancer cells, α2,6-KDN- or α2,6-Neu5Ac-linked *N*-glycans are the dominant species (>98% in total free glycans). Intriguingly, the amount of each free α2,6-KDN-linked *N*-glycan is nearly equal or comparable with that of free α2,6-Neu5Ac-linked *N*-glycan, which has the same pentasaccharide backbone (Table III). Namely, F3-2 and F5-3 are free α2,6-Neu5Ac- and α2,6-KDN-linked *N*-glycans, respectively, having the same pentasaccharide backbone, Galβ1-4GlcNAcβ1-2Manα1-3Manβ1-4-GlcNAc. The amount of F3-2 and F5-3 was ~60 pmol/100 μg protein (i.e. 60.4 and 55.9 pmol/100 μg protein, respectively; Table III). A similar pattern was observed for F4 and F6 (33.0 and 23.4 pmol/100 μg protein), F3-1 and F5-2 (22.9 and 20.8 pmol/100 μg protein) and F5-1 and F7 (3.5 and 7.7 pmol/100 μg protein), in which each pair has a common pentasaccharide backbone. The relative amount of free α2,6-Neu5Ac- and α2,6-KDN-containing *N*-glycans were as follows: F3-2 (25%) >> F4 (14%) > F3-1 (10%) > F5-1 (1%) and F5-3 (23%) >> F6 (10%) > F5-2 (9%) > F7 (3%) (Table III). The profiling of GSLs and free oligosaccharides of the primary prostate cancer lesion of this case is shown in Figure 1B. Although the ratio of KDN-linked free *N*-glycans was slightly lower than those of the metastatic lesion, profiles of free oligosaccharides from the two lesions, primary and metastatic, seem to be similar (Figure 1A and B, Table III).

The ratio of free KDN-containing oligosaccharides of the other three cases was much less than that of the previous case, as detailed below (Figure 1C–E). In the case (case 5, Supplementary data, Table S1) shown in Figure 1C, in group 1 and group 2 free *N*-glycans, four peaks, F3, F4, F5 and F6,

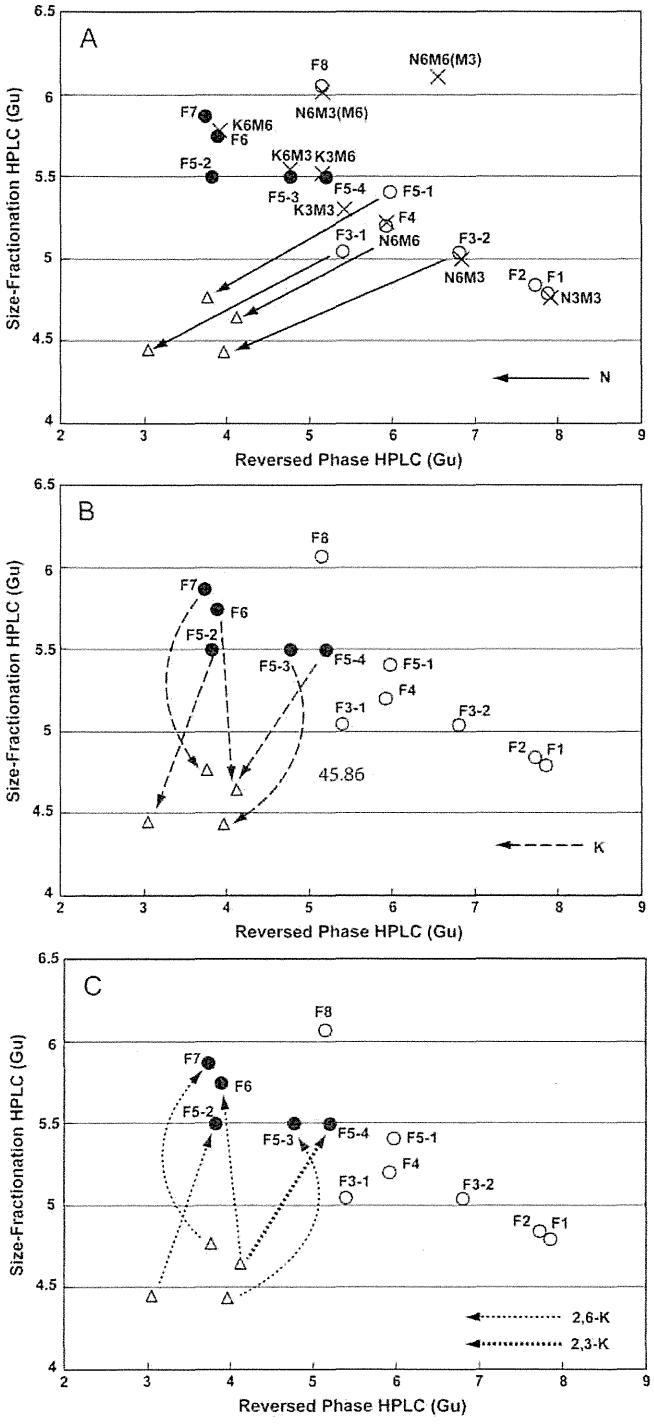

Fig. 2. Digestion of PA-oligosaccharides with *N*-acetylneuraminidase and KDNase and transfer of KDN to desialylated oligosaccharides by sialyltransferases. The elution profiles of PA-*N*-glycans are summarized in the form of a 2D map. Xs in (**A**) indicate the positions of the authentic PA-*N*-glycans (Table I). Open circles indicate the positions of free Neu5Ac-containing *N*-glycans, F1, F2, F3-1, F3-2, F4, F5-1 and F8. Closed circles indicate the positions of free KDN-containing *N*-glycans, F5-2, F5-3, F5-4, F6 and F7. Triangles indicate the positions of the digested products with sialidase and KDNase. (A) Lines indicate the direction of the change after *N*-acetylneuraminidase digestions of F3-1, F3-2, F4 and F5-1 (abbreviated as N). (**B**) Broken lines indicate the direction of the change after KDNase digestions of F5-2, F5-3, F5-4, F6 and F7 (abbreviated as K). (**C**) Thin dotted lines and the thick dotted line indicate the change after transfer of KDN by α2,6-sialyltransferase (abbreviated as 2,6-K) and α2,3-sialyltransferase (abbreviated as 2,3-K) to the desialylated products, respectively. In (B) and (C), mark Xs (positions of standard glycans) are omitted, and two lines are curved so as not cross the irrelevant marks.

composed of seven glycans, F3-1, F3-2, F4, F5-1, F5-2, F5-3 and F6, were observed (Figure 1C). The amount of free Neu5Ac-containing *N*-glycans, F3-1, F3-2, F4 and F5-1, was similar or comparable with those of the previous case shown in Figure 1A and B, but the amount of free KDN-containing *N*-glycans, F5-2, F5-3 and F6, was quite low (Table III). Furthermore, F7, which was the major component of the previous case, was not found. In the cases shown in Figure 1D and E (cases 3 and 4, respectively, Supplementary data, Table S1), both Neu5Ac-containing and KDN-containing free *N*-glycans were much lower than those of the case shown in Figure 1A and B (Table III). No correlation was found between the amounts of free oligosaccharides and the clinicopathological features of the four cases.

Discussion

We recently reported that large amounts of free Neu5Ac-containing complex-type *N*-glycans accumulate in pancreatic cancers (Yabu et al. 2013). In contrast, only trace amounts of these *N*-glycans were detected in colorectal cancer tissue (Yabu et al. 2013).

Surprisingly, in addition to the free Neu5Ac-containing *N*-glycans, substantial amounts of free KDN-containing *N*-glycans were found to have accumulated in prostate cancers. To date, elevated expression of free KDN has been reported in fetal human red blood cells compared with adult red blood cells and ovarian tumor tissues compared with normal controls (Inoue et al. 1998). KDN-rich glycoproteins were isolated from PA-1 cells, which were partially purified and characterized (Inoue et al. 2006). Here, we demonstrate the substantial accumulation of KDN glycoconjugates in human prostate cancer tissues in the form of free complex-type *N*-glycans. Moreover, the structures of these molecules have been investigated in detail.

The characteristic features of free Neu5Ac- and KDN-containing *N*-glycans associated with human prostate cancers can be summarized as follows: (i) most of the free *N*-glycans were composed of α2,6-Neu5Ac- or α2,6-KDN-linked glycans, (ii) the branch on the α6-Man arm of biantennary *N*-glycans was preferentially removed. These features were also observed in the Neu5Ac-containing free *N*-glycans accumulated in human pancreatic and colorectal cancers (Yabu et al. 2013). These data suggest a common mechanism among the various human cancers that underlies the accumulation of free complex-type *N*-glycans.

Our findings raise three important questions concerning the generation and degradation of KDN-containing glycoconjugates. First, do free KDN-containing *N*-glycans accumulate as a result of insufficient degradation (e.g. insufficient lysosomal function) or overproduction of KDN-containing *N*-glycans,

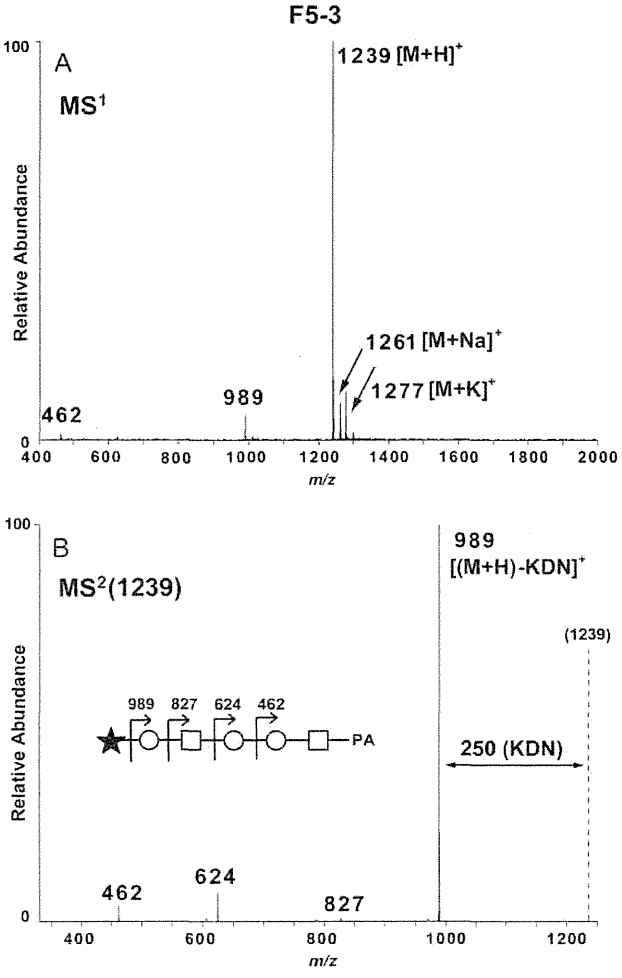

Fig. 3. $MS^{1,2}$ spectra of F5-3. (**A**) MS^1 spectra of F5-3; (**B**) MS^2 spectra of $[M+H]^+$ precursor ion at *m/z* 1239 detected in MS^1 of (A). The MS^2 fragment ions were assigned as shown schematically. Symbol representations of glycans are as follows: Hex, open circles; HexNAc, open squares; KDN, closed star.

which exceeds normal degradation capacity, leading to the accumulation of KDN-containing *N*-glycans? The former mechanism was proposed to be responsible for the accumulation of free Neu5Ac-containing *N*-glycans in human stomach cancer-derived cell lines, MKN7 and MKN45 cells (Ishizuka et al. 2008). Our preliminary analysis of the structures of membrane-bound glycoprotein *N*-glycans of a couple of prostate cancer tissues, including the case shown in Figure 1A in which the levels of free Neu5Ac- and KDN-containing *N*-glycans were almost the same, may provide an important clue to answer this question. From these analyses, all the acidic *N*-glycans were composed of Neu5Ac-linked *N*-glycans, and no KDN-linked *N*-glycans have been observed in membrane-bound glycoprotein *N*-glycans, even though more than 99% of total acidic membrane-bound glycoprotein *N*-glycans was analyzed by MS^2. These results suggest that the free KDN-containing *N*-glycans accumulate because of insufficient degradation, rather than overproduction.

The second question is whether sialidases that are able to cleave KDN linkages are present in human? In general, KDN linkages are resistant to the action of bacterial and viral sialidases, with one exception of that derived from *Sphingobacterium multivorum* (Kitajima et al. 1994). Sialidases that cleave both KDN and Neu5Ac linkages (KDN sialidases) have been reported in animals that contain rich KDN glycoconjugates, such as rainbow trout (Angata et al. 1994). Currently, four kinds of human neuraminidases, Neu1 (lysosomal), Neu2 (cytosolic), Neu3 and Neu4 (both membrane-bound), are known to mediate the release of an Neu5Ac residue from sialoglyconjugates (Achyuthan and Achyuthan 2001; Monti et al. 2004). KDN linkages are thought to be resistant to the action of human sialidases, because biochemical analyses revealed that mammalian Neu1, Neu2 and Neu4 could not cleave KDN linkages (Davies et al. 2012; Sato and Kitajima, unpublished results). However, further studies will be needed to clarify the mechanism responsible for the preferential accumulation of free α2,6-linked KDN *N*-glycans and the preferential removal of the α6-Man arm of the *N*-glycan core structures.

The third question arising from our findings is why free KDN-containing *N*-glycans accumulate specifically in prostate cancers, but not in normal and cancerous tissues from the colon and pancreas? The abundance of KDN in prostate cancer tissues is thought to be very low, probably less than 1% of total sialic acid content according to our structural analyses of membrane-bound glycoprotein *N*-glycans. Nonetheless, the level of KDN in prostate cancer tissues might be higher than that of other tissues. The formation of KDN monosaccharide appears to be one of the key factors limiting the biosynthesis of KDN-containing glycoconjugates. Cellular levels of free KDN were found to increase when mouse melanoma B16 and COS-7 cells were cultured in mannose-rich media (mannose being a precursor in the de novo synthesis of KDN) and when human cancer cell lines, HeLa, LS174T and Caco-2 cells, were cultured under hypoxic conditions that mimic the microenvironment inside tumor tissues (Angata et al. 1999; Go et al. 2007). Indeed, specific conditions, such as the hypoxic microenvironment found in prostate cancers, might lead to an increase in the cellular KDN levels.

A defect in glycoprotein degradation by loss of lysosomal glycosidase activity in inherited diseases, such as sialidosis and fucosidosis, leads to the accumulation of partially degraded fragments in tissues and the appearance of related fragments in the urine (Tsay et al. 1976; Strecker et al. 1977). Three kinds of Neu5Ac-containing *N*-glycans that accumulate in prostate cancers, F3-2, F1 and F8, are present in the urine of patients with the lysosomal disease, sialidosis (Strecker et al. 1977). Hence, it is possible that the levels of free Neu5Ac- and KDN-containing *N*-glycans might be increased in the urine of prostate cancer patients.

In summary, this is the first study to report the identification and characterization of KDN as a glycoconjugate in human tissues. We have unequivocally demonstrated that substantial amounts of free KDN-containing complex-type *N*-glycans accumulate in prostate cancers. To evaluate free KDN-containing *N*-glycans as potential tumor markers, the levels of these oligosaccharides in the urine of prostate cancers and normal controls must be assessed.

Materials and methods

All human tissue specimens were obtained from Osaka University Medical School-related hospital. This study was approved by the Local Ethics Committee of Osaka Medical Center for Cancer and Cardiovascular Diseases. Informed consent was obtained from each patient. Primary and metastatic prostate cancerous tissue samples were used in this study. Most of the samples were needle biopsies. Normal prostate tissues were not examined due to the difficulty of obtaining normal prostate tissues from biopsy samples. The majority of the experimental procedures used in this study have been reported previously, including the isolation of GSLs and free oligosaccharides, preparation and separation of PA-oligosaccharides and mass spectrometry analyses (Misonou et al. 2009). In brief, prostate cancer tissues were extracted with 1200 μL of chloroform/methanol (2:1, v/v), followed by 800 μL of chloroform/methanol/water (1:2:0.8, v/v/v). This methodology extracts both GSLs and free oligosaccharides. The extracts were loaded onto a DEAE-Sephadex A25 column and flow-through fractions were collected as neutral oligosaccharides. Acidic oligosaccharides were subsequently eluted with 200 mM ammonium acetate in methanol. The neutral and acidic fractions were digested with recombinant endoglycoceramidase II from *Rhodococcus* Sp. (Takara Bio Inc., Shiga, Japan) to release the oligosaccharide portion from GSLs. Liberated oligosaccharides from GSLs and free oligosaccharides were then labeled with 2-AP (Natsuka and Hase 1998).

PA-oligosaccharides were separated on a Shimadzu LC-20A HPLC system equipped with a Waters 2475 fluorescence detector. Normal-phase HPLC was performed on a TSK gel Amide-80 column (0.2 × 25 cm, Tosoh, Tokyo, Japan). The molecular size of each PA-oligosaccharide is given in glucose units (Gu) based on the elution times of PA-isomaltooligosaccharides. Reverse-phase HPLC was performed on a TSK gel octa decyl silyl (ODS)-80Ts column (0.2 × 15 cm, Tosoh). The retention time of each PA-oligosaccharide is given in Gu based on the elution times of PA-isomaltooligosaccharides. Thus, a given compound on these two columns provides a unique set of Gu (amide) and Gu (ODS) values, which correspond to coordinates of the 2D map. PA-oligosaccharides were analyzed by LC/ESI MS^2 according to our previously established procedures (Korekane et al. 2007).

Glycosidase digestions

KDN-linked PA-oligosaccharides were digested with 2 U/mL of KDNase from *S. multivorum*, which specifically hydrolyzes deaminoneuraminyl but not *N*-acetylneuraminyl linkages, in 100 mM Tris-acetate buffer, pH 6.0 containing 100 mM NaCl and 0.1% bovine serum albumin for 16 h at 25°C (Kitajima et al. 1994; Nishino et al. 1996). PA-oligosaccharides were digested with 2 U/mL of α-sialidase from *Arthrobacter ureafaciens* (Nacalai, Nakagyo-ku, Kyoto, Japan) in 100 mM sodium acetate buffer, pH 5.5, for 2 h at 37°C.

Preparation of KDN-containing standard glycans from Neu5Ac-containing standard glycans

Neu5Acα2-6Galβ1-4GlcNAcβ1-2Manα1-6Manβ1-4GlcNAc-PA (N6M6, Table I), Neu5Acα2-6Galβ1-4GlcNAcβ1-2Manα1-3Manβ1-4GlcNAc-PA (N6M3, Table I) and two kinds of Neu5Acα2-6Galβ1-4GlcNAcβ-Manα-Manβ1-4GlcNAc obtained in this study (F3-1 and F5-1 in Table III, probably Neu5Acα2-6Galβ1-4GlcNAcβ1-6Manα1-6Manβ1-4GlcNAc and Neu5Acα2-6Galβ1-4GlcNAcβ1-4Manα1-3Manβ1-4GlcNAc) were treated with α-sialidase from *A. ureafaciens*. KDN was enzymatically transferred to the non-reducing terminal Gal residue of the four kinds of desialylated free complex-type *N*-glycans via α2,3- and α2,6-linkages using CMP-KDN as the donor substrate. The glycosyltransferases used in these reactions were purified rat α2,3-sialyltransferase (Merck, Darmstadt, Germany) and human α2,6-sialyltransferase I recombinant protein. The latter enzyme was engineered for expression and purified as described in our previous study (Korekane et al. 2010). The incubation mixture contained the following components in a total volume of 10 μL: cacodylate buffer, pH 6.5, 10 mM $MnCl_2$, 0.45% Triton X-100, 2 mM CMP-KDN, 1 μL of enzyme source and an appropriate amount of each acceptor substrate. After incubation at 37°C for 16 h, the reaction mixtures were subjected to normal-phase HPLC. The fractions containing KDN-linked PA-oligosaccharides were then subjected to mass spectrometry analysis and reverse-phase HPLC to determine Gu. The structures and Gu of KDN-containing authentic PA-oligosaccharides are listed in Table I.

Supplementary data

Supplementary data for this article is available online at http://glycob.oxfordjournals.org/.

Funding

This work was supported in part by Grant-in-Aid for Scientific Research (C) (23501303) from the Ministry of Education, Culture, Sports, Science and Technology of Japan and by the Program for Promotion of Fundamental Studies in Health Sciences of the National Institute of Biomedical Innovation (NIBIO).

Acknowledgements

This study was performed in part as a research program of the Project for Development of Innovative Research on Cancer Therapeutics (P-Direct), Ministry of Education, Culture, Sports, Science and Technology of Japan.

Conflict of interest

None declared.

Abbreviations

2-AP, 2-aminopyridine; 2D, two-dimensional; CMP-KDN, cytidine monophospho-KDN; ESI, electrospray ionization; GSL, glycosphingolipid; Gu, glucose units; HPLC, high-performance liquid chromatography; LC, liquid chromatography; LST, LS tetrasaccharide; KDN, 2-keto-3-deoxy-D-*glycero*-D-*galacto*-nononic acid; ODS, octa decyl silyl; Neu5Ac, *N*-acetylneuraminic acid; PA, pyridylaminated.

References

Achyuthan KE, Achyuthan AM. 2001. Comparative enzymology, biochemistry and pathophysiology of human exo-alpha-sialidases (neuraminidases). *Comp Biochem Physiol B Biochem Mol Biol.* 129(1):29–64.

Alley WR, Jr, Vasseur JA, Goetz JA, Svoboda M, Mann BF, Matei DE, Menning N, Hussein A, Mechref Y, Novotny MV. 2012. N-linked glycan structures and their expressions change in the blood sera of ovarian cancer patients. *J Proteome Res.* 11(4):2282–2300.

Angata T, Kitajima K, Inoue S, Chang J, Warner TG, Troy FA, 2nd, Inoue Y. 1994. Identification, developmental expression and tissue distribution of deaminoneuraminate hydrolase (KDNase) activity in rainbow trout. *Glycobiology.* 4(4):517–523.

Angata T, Nakata D, Matsuda T, Kitajima K. 1999. Elevated expression of free deaminoneuraminic acid in mammalian cells cultured in mannose-rich media. *Biochem Biophys Res Commun.* 261(2):326–331.

Brockhausen I. 1999. Pathways of O-glycan biosynthesis in cancer cells. *Biochim Biophys Acta.* 1473(1):67–95.

Davies LR, Pearce OM, Tessier MB, Assar S, Smutova V, Pajunen M, Sumida M, Sato C, Kitajima K, Finne J, et al. 2012. Metabolism of vertebrate amino sugars with N-glycolyl groups: Resistance of alpha2-8-linked N-glycolylneuraminic acid to enzymatic cleavage. *J Biol Chem.* 287 (34):28917–28931.

Go S, Sato C, Yin J, Kannagi R, Kitajima K. 2007. Hypoxia-enhanced expression of free deaminoneuraminic acid in human cancer cells. *Biochem Biophys Res Commun.* 357(2):537–542.

Hakomori S. 2002. Glycosylation defining cancer malignancy: New wine in an old bottle. *Proc Natl Acad Sci USA.* 99(16):10231–10233.

Inoue S, Kitajima K. 2006. KDN (deaminated neuraminic acid): Dreamful past and exciting future of the newest member of the sialic acid family. *Glycoconj J.* 23(5–6):277–290.

Inoue S, Kitajima K, Inoue Y. 1996. Identification of 2-keto-3-deoxy-D-glycero—galactonononic acid (KDN, deaminoneuraminic acid) residues in mammalian tissues and human lung carcinoma cells. Chemical evidence of the occurrence of KDN glycoconjugates in mammals. *J Biol Chem.* 271 (40):24341–24344.

Inoue S, Lin SL, Chang T, Wu SH, Yao CW, Chu TY, Troy FA, 2nd, Inoue Y. 1998. Identification of free deaminated sialic acid (2-keto-3-deoxy-D-glycero-D-galacto-nononic acid) in human red blood cells and its elevated expression in fetal cord red blood cells and ovarian cancer cells. *J Biol Chem.* 273(42):27199–27204.

Inoue S, Poongodi GL, Suresh N, Chang T, Inoue Y. 2006. Identification and partial characterization of soluble and membrane-bound KDN(deaminoneuraminic acid)-glycoproteins in human ovarian teratocarcinoma PA-1, and enhanced expression of free and bound KDN in cells cultured in mannose-rich media. *Glycoconj J.* 23(5–6):401–410.

Ishizuka A, Hashimto Y, Naka R, Kinoshita M, Kakehi K, Seino J, Funakoshi Y, Suzuki T, Kameyama A, Narimatsu H. 2008. Accumulation of free complex-type N-glycans in MKN7 and MKN45 stomach cancer cells. *Biochem J.* 413(2):227–237.

Kannagi R, Izawa M, Koike T, Miyazaki K, Kimura N. 2004. Carbohydrate-mediated cell adhesion in cancer metastasis and angiogenesis. *Cancer Sci.* 95(5):377–384.

Kim YJ, Varki A. 1997. Perspectives on the significance of altered glycosylation of glycoproteins in cancer. *Glycoconj J.* 14(5):569–576.

Kitajima K, Kuroyanagi H, Inoue S, Ye J, Troy FA, 2nd, Inoue Y. 1994. Discovery of a new type of sialidase, "KDNase," which specifically hydrolyzes deaminoneuraminyl (3-deoxy-D-glycero-D-galacto-2-nonulosonic acid) but not N-acylneuraminyl linkages. *J Biol Chem.* 269 (34):21415–21419.

Korekane H, Matsumoto A, Ota F, Hasegawa T, Misonou Y, Shida K, Miyamoto Y, Taniguchi N. 2010. Involvement of ST6Gal I in the biosynthesis of a unique human colon cancer biomarker candidate, alpha2,6-sialylated blood group type 2H (ST2H) antigen. *J Biochem.* 148(3):359–370.

Korekane H, Tsuji S, Noura S, Ohue M, Sasaki Y, Imaoka S, Miyamoto Y. 2007. Novel fucogangliosides found in human colon adenocarcinoma tissues by means of glycomic analysis. *Anal Biochem.* 364(1):37–50.

Lau KS, Dennis JW. 2008. N-Glycans in cancer progression. *Glycobiology.* 18(10):750–760.

Misonou Y, Shida K, Korekane H, Seki Y, Noura S, Ohue M, Miyamoto Y. 2009. Comprehensive clinico-glycomic study of 16 colorectal cancer specimens: Elucidation of aberrant glycosylation and its mechanistic causes in colorectal cancer cells. *J Proteome Res.* 8(6):2990–3005.

Monti E, Bassi MT, Bresciani R, Civini S, Croci GL, Papini N, Riboni M, Zanchetti G, Ballabio A, Preti A, et al. 2004. Molecular cloning and characterization of NEU4, the fourth member of the human sialidase gene family. *Genomics.* 83(3):445–453.

Nadano D, Iwasaki M, Endo S, Kitajima K, Inoue S, Inoue Y. 1986. A naturally occurring deaminated neuraminic acid, 3-deoxy-D-glycero-D-galacto-nonulosonic acid (KDN). Its unique occurrence at the nonreducing ends of oligosialyl chains in polysialoglycoprotein of rainbow trout eggs. *J Biol Chem.* 261(25):11550–11557.

Narimatsu H, Sawaki H, Kuno A, Kaji H, Ito H, Ikehara Y. 2010. A strategy for discovery of cancer glyco-biomarkers in serum using newly developed technologies for glycoproteomics. *FEBS J.* 277(1):95–105.

Natsuka S, Hase S. 1998. Analysis of N- and O-glycans by pyridylamination. *Methods Mol Biol.* 76:101–113.

Nishino S, Kuroyanagi H, Terada T, Inoue S, Inoue Y, Troy FA, Kitajima K. 1996. Induction, localization, and purification of a novel sialidase, deaminoneuraminidase (KDNase), from *Sphingobacterium multivorum*. *J Biol Chem.* 271(6):2909–2913.

Peracaula R, Barrabes S, Sarrats A, Rudd PM, de Llorens R. 2008. Altered glycosylation in tumours focused to cancer diagnosis. *Dis Markers.* 25(4–5):207–218.

Saldova R, Wormald MR, Dwek RA, Rudd PM. 2008. Glycosylation changes on serum glycoproteins in ovarian cancer may contribute to disease pathogenesis. *Dis Markers.* 25(4–5):219–232.

Shida K, Korekane H, Misonou Y, Noura S, Ohue M, Takahashi H, Ohigashi H, Ishikawa O, Miyamoto Y. 2010. Novel ganglioside found in adenocarcinoma cells of Lewis-negative patients. *Glycobiology.* 20(12):1594–1606.

Shida K, Misonou Y, Korekane H, Seki Y, Noura S, Ohue M, Honke K, Miyamoto Y. 2009. Unusual accumulation of sulfated glycosphingolipids in colon cancer cells. *Glycobiology.* 19(9):1018–1033.

Strecker G, Peers MC, Michalski JC, Hondi-Assah T, Fournet B, Spik G, Montreuil J, Farriaux JP, Maroteaux P, Durand P. 1977. Structure of nine sialyl-oligosaccharides accumulated in urine of eleven patients with three different types of sialidosis. Mucolipidosis II and two new types of mucolipidosis. *Eur J Biochem.* 75(2):391–403.

Tsay GC, Dawson G, Sung SS. 1976. Structure of the accumulating oligosaccharide in fucosidosis. *J Biol Chem.* 251(19):5852–5859.

Yabu M, Korekane H, Takahashi H, Ohigashi H, Ishikawa O, Miyamoto Y. 2013. Accumulation of free Neu5Ac-containing complex-type N-glycans in human pancreatic cancers. *Glycoconj J.* 30(3):247–256.

Journal of proteome research

Article

pubs.acs.org/jpr

Analysis of Polarized Secretion of Fucosylated Alpha-Fetoprotein in HepG2 Cells

Tsutomu Nakagawa,[†] Kenta Moriwaki,[†] Naoko Terao,[†] Takatoshi Nakagawa,[‡] Yasuhide Miyamoto,[§] Yoshihiro Kamada,[†] and Eiji Miyoshi*[,†]

[†]Department of Molecular Biochemistry and Clinical Investigation, Osaka University Graduate School of Medicine, Osaka, Japan

[‡]Department of Pharmacology, Osaka Medical College, Osaka, Japan

[§]Department of Immunology, Osaka Medical Center for Cancer and Cardiovascular Diseases, Osaka, Japan

ABSTRACT: Fucosylated alpha-fetoprotein (AFP) is a more specific biomarker for hepatocellular carcinoma (HCC) than AFP. However, the mechanisms underlying the increase in fucosylated AFP in sera of HCC patients remain largely unknown. Recently, we reported that fucosylation is a possible signal for the secretion of hepatic glycoproteins into bile and that the fucosylation-based sorting machinery might be disrupted in the liver bearing HCC. In this study, we investigated the selective secretion of fucosylated AFP into bile canaliculus (BC) structures of the human hepatoma cell line HepG2. The proportion of fucosylated AFP in BC structures was higher than that in the medium, as judged by lectin affinity electrophoresis. Suppression of fucosylation by the double knock-down of GDP-mannose-4,6-dehydratase and the human homologue of GDP-4-keto-6-deoxymannose-3,5-epimerase-4-reductase, which contribute to the synthesis of GDP-fucose, a donor substrate for fucosyltransferases, did not decrease the proportion of fucosylated AFP in BC structures but decreased this proportion in conditioned medium. Furthermore, increased AFP fucosylation was observed in medium, but not in BC structures, upon adding free fucose. These results suggest that saturation of fucosylated AFP in BC structures is accompanied by its increase in conditioned medium, probably leading to increased fucosylated AFP in sera of HCC patients.

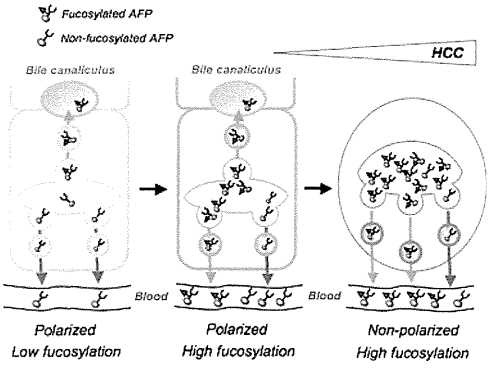

KEYWORDS: *AFP-L3, fucose, bile canaliculus, HepG2 cells*

INTRODUCTION

Alpha-fetoprotein (AFP) is an oncofetal glycoprotein that contains a single *N*-glycosylation site,[1] and its oligosaccharide structure varies with developmental stage and disease state.[2−4] Fucosylated AFP, referred to as the L3 fraction of AFP (AFP-L3), is a highly specific tumor marker for hepatocellular carcinomas (HCC). Increases in serum AFP levels are observed in patients with chronic liver diseases such as liver cirrhosis, but fucosylated AFP is scarcely detected in benign liver disease.[5] The majority of the oligosaccharide structures of AFP-L3 are alpha1−6 fucosylated biantennary structures.[4] Alpha1−6 fucosyltransferase (Fut8) is involved in the fucosylation of AFP, and we previously succeeded in the purification and cDNA cloning of Fut8 from porcine brain[6] and a human gastric cancer cell line.[7] Whereas overexpression of Fut8 in Hep3B cells increased the rate of fucosylation of AFP, high expression of Fut8 was observed in noncancerous liver cirrhotic tissues as well as in HCC tissues.[8] Therefore, other factors must be linked to the specific incidence of fucosylated AFP in HCC. GDP-fucose is a donor substrate for Fut8. When we determined the GDP-fucose levels in liver tissues, using an assay for GDP-fucose levels in cells/tissues, the levels in HCC tissues were found to be significantly higher than those in cirrhotic and normal liver tissues.[9,10] The increase in GDP-fucose in HCC is due to the enhanced expression of the human homologue of GDP-4-keto-6-deoxymannose-3,5-epimerase-4-reductase (FX), which contributes to the synthesis of GDP-fucose.[11] Therefore, both Fut8 and FX would regulate the production of fucosylated AFP in HCC. However, Fut8 and FX were increased 2- to 3-fold in HCC tissues compared to the surrounding tissues, and thus another factor must be involved in terms of an increase in fucosylated AFP in the sera of HCC patients.

Hepatocytes, the major epithelial cells in the liver, produce a variety of serum glycoproteins and nonglycosylated proteins including albumin. There are two secretion pathways in hepatocytes. One pathway involves secretion to the apical surface of hepatocytes, which is followed by secretion into bile ducts. The other involves secretion to the basolateral surface, which is followed by secretion into blood vessels. Interestingly, it is reported that common serum proteins including albumin are detected in bile.[12] The molecular and cellular mechanisms for the secretion pathway are intensively investigated topics, but remain largely unknown.

Recently, we reported that many glycoproteins in bile were strongly fucosylated, compared to those in serum, and

Received: November 22, 2011
Published: April 9, 2012

suggested that fucosylation might be a possible signal for the secretion of glycoproteins into bile.[13] Further, we found that the sorting machinery via fucosylation might be disrupted in a rodent HCC model.[14] The question therefore arises whether fucosylated AFP is also regulated by this common fucosylation sorting system.

In this study, to investigate the polarized secretion of fucosylated AFP in the HCC liver, we used human hepatocarcinoma (HepG2) cells, which form bile canaliculus (BC) structures[15,16] and produce fucosylated AFP. Polarized HepG2 cells have been proven to be a suitable model for the study of several functional properties of normal hepatocytes, including metabolism, sorting, polarized transport, and secretion.[17] Glycoproteins secreted into BC structures and the culture medium are equivalent to biliary and serum glycoproteins, respectively. The percentage of fucosylated AFP in BC structures was found to be higher than that in medium. Suppression of fucosylation by double knock-down of GDP-mannose-4, 6-dehydratase (GMD), and FX did not decrease the percentage of fucosylated AFP in BC structures but did decrease the percentage in the medium. Furthermore, the addition of free fucose caused an increase in fucosylation only in AFP secreted into the medium. These results suggested that fucosylated AFP might be secreted into BC structures by the sorting machinery via fucosylation and that the secretion of fucosylated AFP into the medium might be due to the saturation of fucosylated glycoprotein secretion into BC structures.

EXPERIMENTAL SECTION

Reagents

Biotinated AOL (*Aspergillus oryzae*) was purchased from Tokyo Kasei Kogyo Co., Ltd. (Tokyo, Japan). Fucose was from Sigma (St Louis, MO).

Cell Cultures

Cells of the human HCC cell line HepG2 (American Type Culture Collection, Rockville, MD) were cultured in Dulbecco's modified Eagle's medium containing 4.5 g/L of glucose supplemented with 10% fetal bovine serum (FBS), 100 U/mL of penicillin G, and 100 μg/mL of streptomycin in a humidified atmosphere of 5% CO_2 at 37 °C. The formation of BC structures was confirmed by immunostaining for canalicular membrane proteins such as multidrug resistance protein 1, tight junction associated protein, Zonula occludens 1, and actin filaments, with confocal microscopy (data not shown).

The collection of proteins secreted into BC structures was performed by means of the modified method described by Bastaki et al.[18] Briefly, HepG2 cells were seeded at 2.5×10^3 cells/cm^2 on collagen type I-coated dishes (Iwaki, Chiba, Japan) and cultured for 4 days. After the cells were rinsed twice with medium without FBS, the cells were cultured in medium without FBS for 1 day. The medium was collected, and then the cells were incubated twice with 2.5 mM EGTA, 50 mM 2-deoxyglucose, and 5 mM NaN_3 for 15 min at 37 °C to disrupt the tight junctions, thereby releasing the proteins secreted into BC structures. We confirmed that actin, a major cytosolic protein, was not contained in the material from BC structures to deny a possibility of cell damages followed by a release of cellular proteins (data not shown).

Establishment of GMD and FX Double Knock-Down Cell Lines

GMD and FX double knock-down (DKD) cell lines were established by retroviral introduction of small hairpin RNA (shRNA) against the *GMDS* and *FX* genes. Briefly, retroviral expression vectors designed to express shRNA targeted to the *GMDS* and *FX* genes were constructed as follows. A 19-nucleotide sequence of the *GMDS* and *FX* genes was inserted in the sense and antisense directions into the pSINsi-hU6 DNA vector (Takara Bio Inc., Shiga, Japan) and RNAi-Ready pSIREN-RetroQ vector (Promega, Madison, WI) containing the human U6 promoter, respectively. The shRNA for *GMDS* was designed to form 19-bp dsRNA with 2 thymine overhangs at both 3′ ends. The targeting sequences of the *GMDS* and *FX* siRNAs used are as follows. *GMDS*, sense: 5′-CGACUUCUA-GAUGCAGUUATT-3′, antisense: 3′-TTGCUGAAGAU-CUACGUCAAU; *FX*, sense: 5′-GAAGUCACCUUUGAUA-CAA-3′, antisense: 5′-CUUCAGUGGAAACUAUGUU-3′. Recombinant retroviruses were generated by cotransfection of a vector mixture, such as the recombinant retrovirus vector, pE-ampho vector (Amphotropic *env*), and the pGP vector (*gag-pol*) into human embryonic kidney 293 cells. Recombinant retrovirus particles containing the target sequences of *GMDS* and *FX* genes were infected into HepG2 cells, and the Geneticin (G418)-resistant clones for GMD and puromycin-resistant clones for FX were selected as stable transfectants.

Lectin Blot Analysis

Lectin blot analysis was performed as described previously.[19] Briefly, 5 μg of proteins were subjected to 12% sodium dodecylsulfate-polyacrylamide gel electrophoresis (SDS-PAGE). After the electrophoresis, the gel was blotted onto a nitrocellulose membrane. The membrane was incubated with 3% bovine serum albumin in Tris-buffered saline (20 mM Tris, 0.5 M NaCl, pH 7.5; TBS) overnight, and then incubated with 1.0 μg/mL of biotinated AOL lectin in TBST (TBS containing 0.05% Tween 20) for 1 h. After washing with TBST, the membrane was incubated with horseradish peroxidase-conjugated avidin (VECTASTAIN ABC kit, Vector Laboratories, Burlingame, CA) for 1 h and then washed with TBST. Staining was performed with ECL Western blot detection reagents (GE Healthcare U.K. Ltd., Buckinghamshire, England).

Lectin Affinity Electophoresis Using LCA Lectin

Lectin affinity electrophoresis using LCA (*Lens culinaris*) lectin was performed with the AFP-L3 Differentiation Kit L (Wako Pure Chemicals, Osaka, Japan) according to the manufacturer's instructions. Briefly, 2-μL samples were subjected to electrophoresis on an agarose gel containing LCA lectin. The separated AFP was transferred to the membrane attached human AFP antibody by antibody-affinity blotting.

Structural Analysis of Oligosaccharides Derived from Glycoproteins in BC Structures and Medium

Preparations of pyridylamino (PA)-oligosaccharides were performed with BlotGlyco (Sumitomo Bakelite Co., Ltd., Tokyo, Japan) according to the manufacturer's instructions. Structural analyses of PA-oligosaccharides derived from glycoproteins in BC structures and medium were performed by means of the modified method described previously.[14] Briefly, sialic acid moieties on the purified PA-oligosaccharides were removed by neuraminidase treatment (*Arthrobacter ureafaciens*, Nacalai Tesque, Kyoto, Japan) in 0.2 M acetate buffer, pH 7.4, at 37 °C overnight. The asialo PA-

oligosaccharides were separated by reversed-phase high performance liquid chromatography (HPLC) on a Shim-pack CLC-ODS column (Shimadzu Corp., Kyoto, Japan) and subsequent normal phase HPLC on a TSK-gel Amide-80 column (Tosoh Corp., Tokyo, Japan). Elution and detection of PA-oligosaccharides were performed as described by Tomiya et al.[20] The structures of PA-oligosaccharides were determined from the elution positions of individual peaks on the basis of the GALAXY database.[21] The structures of PA-oligosaccharides not registered in the GALAXY database were confirmed by liquid chromatography-electrospray ionization- tandem mass spectrometry (LC-ESI-MS/MS).

Mass Spectrometry

PA-oligosaccharides were analyzed by LC-ESI-MS/MS.[22] HPLC was performed on a Paradigm MS4 equipped with a Magic C18 column (0.2 × 50 mm, Michrome BioResource, Auburn, CA). Each PA-oligosaccharide was injected with a flow rate of 2 μL/min for 3 min and eluted with 50% methanol for 10 min. MS analyses were performed using a LCQ ion trap mass spectrometer (Thermo Finnigan, San Jose, CA) equipped with a nanoelectrospray ion source (AMR, Tokyo, Japan). The nanospray voltage was set at 2.0 kV in the positive ion mode. The heated desolvation capillary temperature was set to 200 °C. In the LCQ method file, the LCQ was set to acquire a full MS scan between 1350 and 2700 m/z followed by MS/MS scans in a data-dependent manner.

RESULTS

Comparison of Oligosaccharide Structures on Glycoproteins Secreted into BC Structures and Medium in HepG2 Cells

We compared the oligosaccharide structures on glycoproteins secreted into BC structures with those on glycoproteins secreted into medium by AOL lectin blot analysis. AOL lectin binds fucose residues.[23] As shown in Figure 1, enhanced intensities of AOL binding were observed in glycoproteins secreted into medium, compared with those in glycoproteins secreted into BC structures. This result was contradictory to the results from previous studies, which showed that many glycoproteins in bile were strongly fucosylated,[13,14] suggesting that the fucosylation-based sorting machinery might be disrupted in HepG2 cells.

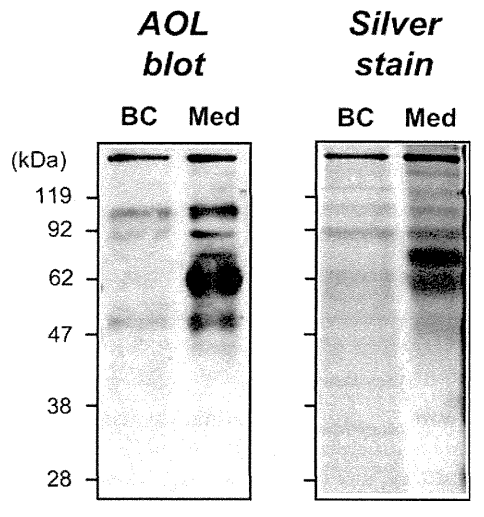

Figure 1. Comparison of the fucosylation levels of glycoproteins secreted into BC structures and into medium. Five micrograms of protein from BC structures and from medium were subjected to silver staining. Lectin blot analysis was performed using the same samples. AOL binds to fucose residues. BC and Med indicate BC structures and medium, respectively. The procedures are described in detail in the Experimental Section.

To determine the oligosaccharide structures on glycoproteins secreted into BC structures and medium in more detail, two-dimensional mapping HPLC and LC-ESI-MS analyses were performed (Table 1). Representative elution profiles of PA-oligosaccharides derived from glycoproteins in BC structures and medium on reversed-phase HPLC are shown in Figure 2. Oligosaccharides specific to BC structures or medium were not observed (Figure 2). As shown in Figure 3, the percentage of peak 7 material on glycoproteins from the medium was larger than that on glycoproteins from BC structures. This result indicated that the enhanced intensities of AOL binding in glycoproteins in the medium might be due to an increase in alpha1−6 fucosylated biantennary structures (peak 7) on glycoproteins.

Determination of the Percentages of Fucosylated AFP Secreted into BC Structures and Medium in HepG2 Cells by LCA-Affinity Electrophoresis

To investigate the polarized secretion of fucosylated AFP in HepG2 cells, the percentages of AFP-L3 in BC structures and medium were determined by LCA-affinity electrophoresis. As shown in Figure 4, the percentage of AFP-L3 in BC structures was higher than that in the medium. This result suggests that fucosylated AFP might be secreted into BC structures preferentially; in other words, AFP might be secreted into BC structures by the sorting machinery via fucosylation.

Suppression of Fucosylation by Double Knock-Down of GMD and FX

As shown in Figure 4, the percentage of fucosylated AFP in medium was also high, although the percentage was smaller than that in BC structures. We previously suggested that the selective secretion of fucosylated glycoproteins into bile might not be disrupted, but might rather be saturated, in the HCC liver in Long-Evans Cinnamon color rats.[14] Therefore, we believed that excess fucosylated glycoproteins, which could not be secreted into BC structures, might be secreted into medium because of the high fucosylation levels in HepG2 cells.

GDP-fucose, a donor substrate for fucosyltransferases, is synthesized via two pathways, the de novo and salvage pathways. The de novo pathway synthesizes GDP-fucose via three reactions catalyzed by GMD and FX, while the salvage pathway synthesizes GDP-fucose from free fucose.[24]

To investigate whether the selective secretion of fucosylated glycoproteins into BC structures is saturated in HepG2 cells, we established cells containing a DKD of GMD and FX. The fucosylation levels in DKD cells should be decreased because of the reduction of GDP-fucose levels. As shown in Figure 5B, fucosylation levels of glycoproteins secreted into the medium in DKD cells were lower than those in wild type. On the other hand, there were no differences between DKD and wild-type cells in the fucosylation levels of glycoproteins secreted into BC structures (Figure 5A).

Next, to rescue the fucosylation levels of glycoproteins in DKD cells, we added 5 mM of free fucose to the medium of DKD cells. The GDP-fucose level is increased via the salvage pathway upon adding free fucose. Increases in fucosylation levels were observed only in glycoproteins secreted into

Table 1. Assignment of the Major PA-Oligosaccharides by Two-Dimensional Mapping HPLC and LC-ESI-MS Analyses

Peak[a]	Structure [b]	ODS[c]	Amide-80[c]	m/z[d]
1		10.3	7.0	1718.9
2	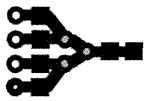	10.3	9.9	2449.5
3	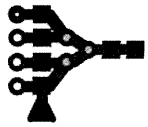	10.3	10.6	2595.2
4	 +▲x2	12.2	8.3	2011.3
5		12.8	8.4	2084.3
6		12.8	9.1	2230.2
7		13.5	7.4	1865.4
8	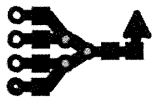	13.5	10.2	2595.2
9	 +▲x3	15.1	9.0	2522.3
10	 +▲x2	16.6	9.5	2376.3
11	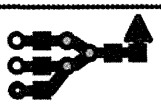	17.0	8.8	2230.2

[a]Numbers at each peak indicated correspond to those in Figures 2, 3, and 6. [b]Monosaccharides were denoted by ○, galactose; ■, *N*-acetylglucosamine; ●, mannose; ▲, fucose. [c]The elution positions on HPLC columns were expressed as glucose units (GU). The chromatographic conditions were described in the Experimental Section. [d]The ions correspond to $[M + H]^+$.

medium upon adding free fucose (Figure 5). Further, we calculated the ratio of peak 7 material to peak 1 material to determine changes in fucosylation level. The percentage of fucosylation in medium was increased upon adding free fucose in DKD cells (Figure 6B). On the other hand, this percentage was almost the same in BC structures in the presence and absence of free fucose in DKD cells (Figure 6A). These results showed that the fucosylated glycoproteins increased in DKD cells upon adding free fucose, and then the glycoproteins were solely secreted into the medium. Taken together, these results suggest that the secretion of fucosylated glycoproteins into BC structures might be saturated in HepG2 cells.

Polarized Secretion of Fucosylated AFP in HepG2 Cells with Different Fucosylation Levels

Peaks 1 and 7 are predominantly composed of the oligosaccharide structures of AFP-L1 and AFP-L3, respectively. The result shown in Figure 6 suggested that the secretion of fucosylated AFP into BC structures might be saturated and that the excess fucosylated AFP might be secreted into medium. To verify this, we compared the percentages of AFP-L3 secreted into BC structures and medium between HepG2 cells with different fucosylation levels by LCA-affinity electrophoresis. As shown in Figure 7B, the percentage of AFP-L3 secreted into medium was decreased in DKD cells, compared with wild-type cells, and an increase in the percentage of AFP-L3 was observed

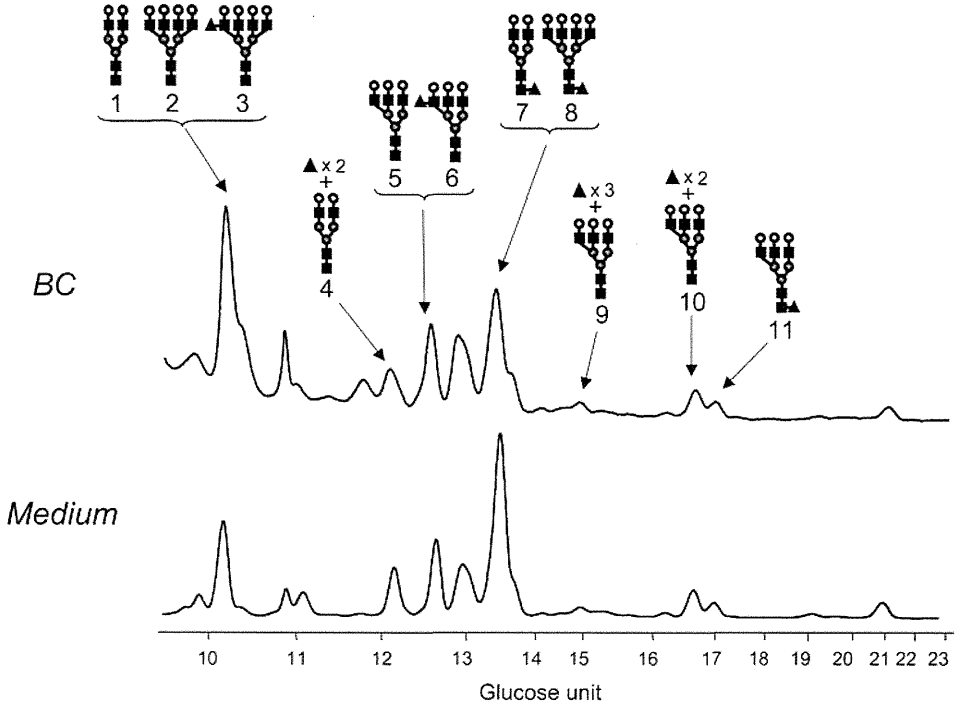

Figure 2. HPLC separation of PA-oligosaccharides derived from glycoproteins in BC structures and medium. Representative elution profiles of PA-oligosaccharides derived from glycoproteins in BC structures (top) and medium (bottom) on an ODS column. The numbers of the peaks and the symbols for monosaccharides correspond to those in Figures 3 and 6 and Table 1. The procedures are described in detail in the Experimental Section.

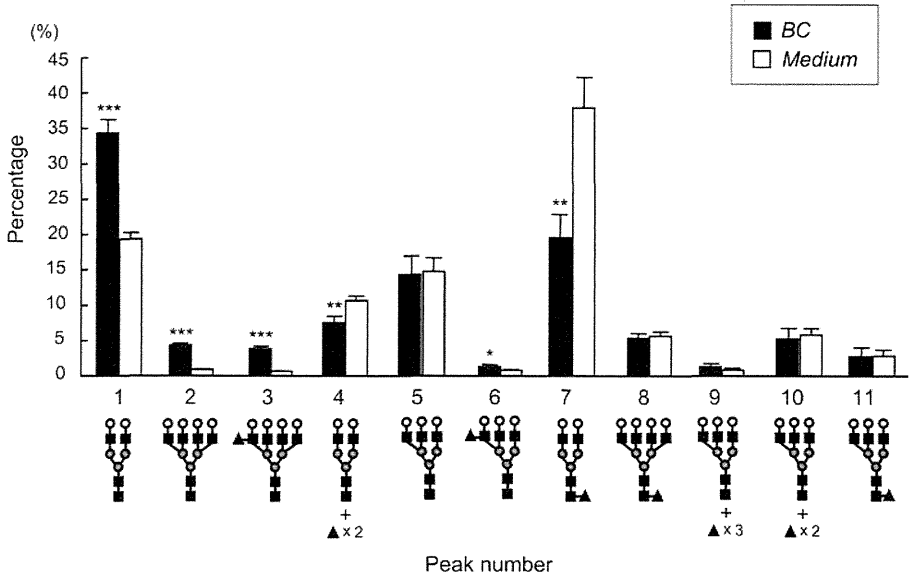

Figure 3. Percentages of oligosaccharide structures on glycoproteins in BC structures and medium. Percentages of each oligosaccharide structure in the total area of the assigned peaks were calculated on the basis of the peak areas from the ODS and Amide-80 elution profiles. The numbers of the peaks and the symbols for monosaccharides correspond to those in Figures 2 and 6 and Table 1. Closed and open columns indicate BC structures and medium, respectively. Each column represents the mean plus SD for three different experiments. *, significantly different ($p < 0.05$) from medium; **, significantly different ($p < 0.01$) from medium; ***, significantly different ($p < 0.001$) from medium.

by adding free fucose in DKD cells. On the other hand, there were no significant differences in the percentages of AFP-L3 secreted into BC structures among these three kinds of cells (Figure 7A).

DISCUSSION

Our previous results suggested that fucosylation is a possible signal for the secretion of glycoproteins into bile in the liver and that the fucosylation-based sorting machinery might be disrupted in hepatocarcinogenesis.[13,14] These findings provide an explanation to the increased level of fucosylated AFP seen in sera of HCC patients. In this study, to investigate the secretion mechanism of fucosylated AFP into bile/serum in detail, we analyzed the selective secretion of fucosylated AFP into BC structures and conditioned medium of HepG2 cells.

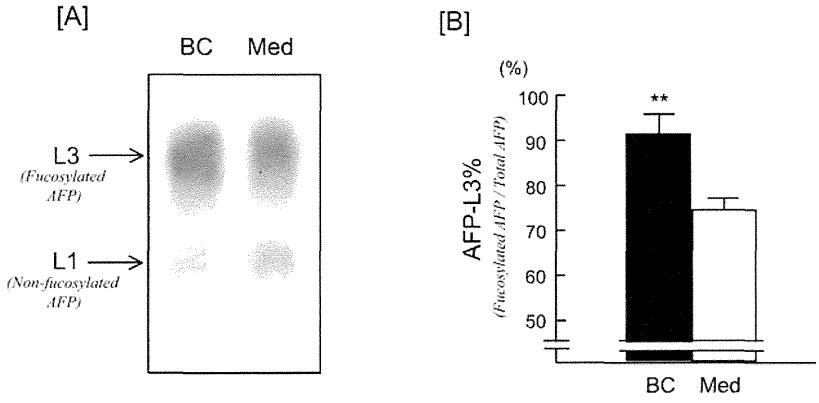

Figure 4. LCA-affinity electrophoresis of AFP secreted into BC structures and medium. AFP in BC structures and medium were subjected to LCA-affinity electrophoresis using an AFP Differentiation Kit L (Wako Pure Chemicals) [A]. The procedures are described in detail in the Experimental Section. The bands corresponding to AFP-L1 (nonfucosylated AFP) and -L3 (fucosylated AFP) are indicated by arrows. BC and Med indicate BC structures and medium, respectively. The proportion of fucosylated AFP in total AFP was calculated as a percentage [B]. Closed and open columns indicate BC structures and medium, respectively. Each column represents the mean plus SD for three different experiments. **, significantly different ($p < 0.01$) from medium.

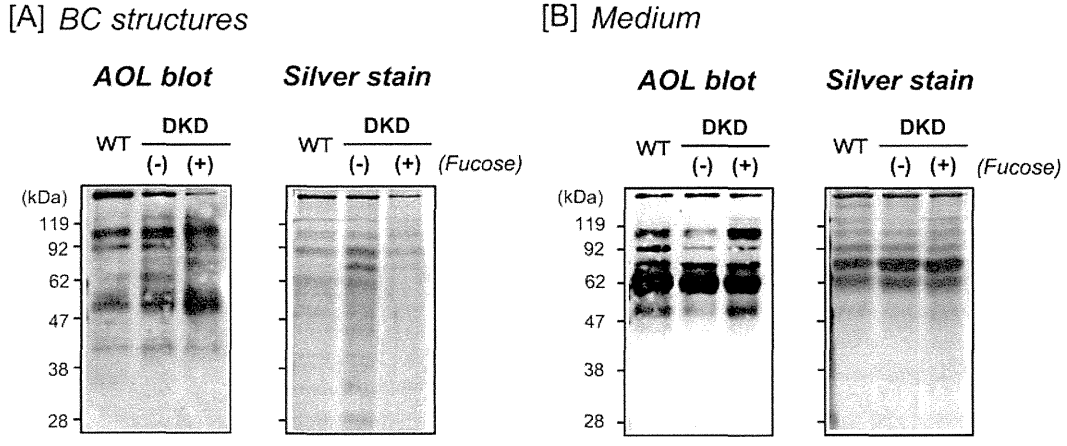

Figure 5. Lectin blot analyses of glycoproteins secreted into BC structures and medium in HepG2 cells with different fucosylation levels. Five micrograms of proteins from BC structures [A] and medium [B] were subjected to silver staining. Lectin blot analyses were performed using the same samples. AOL binds to fucose residues. The procedures are described in detail in the Experimental Section. WT and DKD indicate wild-type cells and cells with a double knock-down of GMD and FX, respectively.

HepG2 cells express high levels of fucosylation regulatory genes, while normal hepatocytes do not express them. Therefore, most of the AFP produced by HepG2 cells is fucosylated AFP (AFP-L3). As expected, greater than approximately 90% of AFP in BC structures was fucosylated, as shown in Figure 4. These data corroborate our hypothesis of fucosylation-based sorting of proteins. Next, we found that suppression of fucosylation by double knock-down of GMD and FX did not reduce the percentage of fucosylated AFP in BC structures, but did decrease the percentage of fucosylated AFP in medium (Figure 7). Furthermore, an increase in fucosylation level was observed in AFP in the conditioned medium, but not in the BC structures, upon adding free fucose (Figure 7). These results suggest that the secretion of fucosylated AFP into BC structures might be saturated in HepG2 cells and that excess fucosylated AFP might be secreted into the medium. This result is consistent with the clinical observation that low levels of AFP-L3 are detected in sera of patients with benign liver disease. More recently, Kuno et al. reported that an increase in fucosylation on serum alpha1-acid glycoprotein (AGP) is associated with liver fibrosis,[25] suggesting that noncancerous hepatocytes with high levels of fucosylation might lead to the saturated secretion of fucosylated proteins into bile. More recently, Hanaoka et al. reported that fucosylated AFP was useful as a prognostic factor for the occurrence of HCC.[26] The results in this study suggest that overexpression of fucosylated proteins is an early event of hepatocarcinogenesis.

Our data from Figure 1 suggest that the selective secretion of most fucosylated glycoproteins into BC structures is disrupted in HepG2 cells. In the absence of such disruption, the fucosylation levels of glycoproteins such as AFP in BC structures should be higher than those in the conditioned medium. It has been reported that an *N*-glycan at a specific site plays a pivotal role in apical sorting in a glycoprotein possessing multiple *N*-glycans.[27] Protein-specific *N*-glycans bearing the responsibility for apical sorting might be involved in selective secretion into bile. Selective secretion via fucosylation of most glycoproteins, with the exception of AFP, might be disrupted in HepG2 cells. Analyses of conformational oligosaccharides on each glycoprotein are required.

We believe that there might be a receptor containing a lectin domain that interacts with fucosylated oligosaccharides and that this receptor could regulate the secretion of soluble

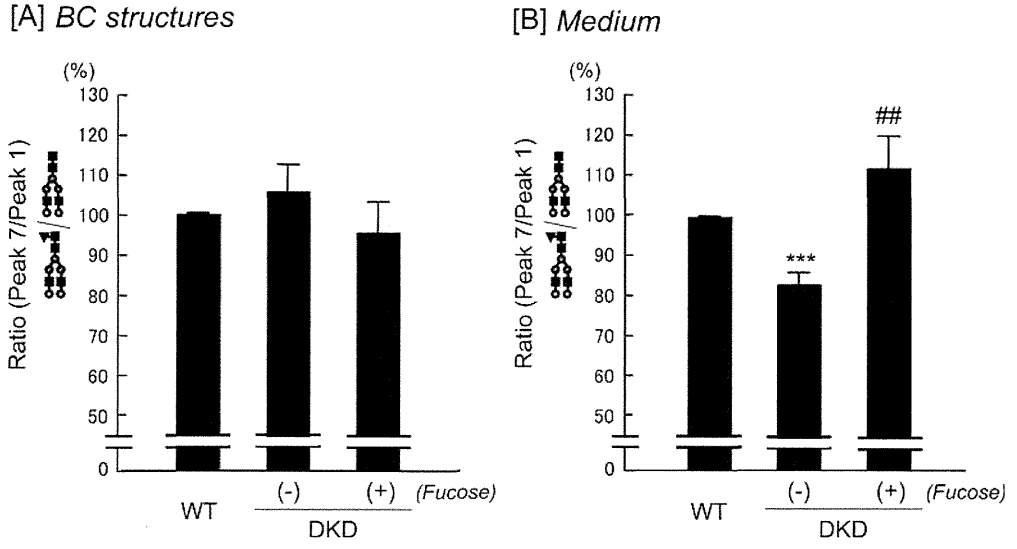

Figure 6. Comparison of the ratio of peak 7 material to peak 1 material between HepG2 cells with different fucosylation levels. The ratio of peak 7 material to peak 1 material from BC structures [A] and medium [B] were calculated on the basis of the peak areas of the ODS and Amide-80 elution profiles, and the values were corrected for that of wild type. The numbers of the peaks and the symbols for monosaccharides correspond to those in Figures 2 and 3 and Table 1. WT and DKD indicate wild-type cells and cells with a double knock-down of GMD and FX, respectively. Each column represents the mean plus SD for three different experiments. ***, significantly different ($p < 0.001$) from wild type; ##, significantly different ($p < 0.01$) from without fucose.

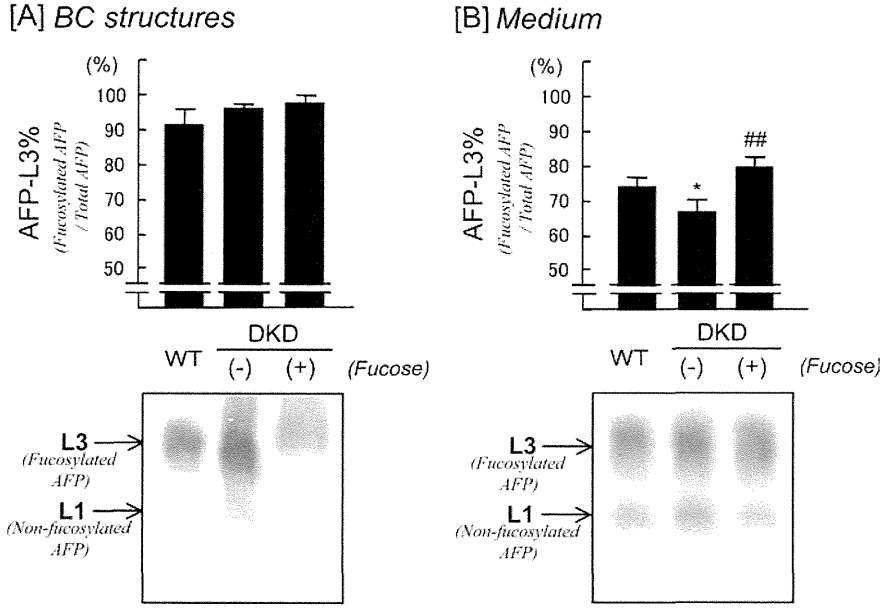

Figure 7. Comparison of the percentages of fucosylated AFP between HepG2 cells with different fucosylation levels. AFP in BC structures [A] and medium [B] from HepG2 cells with three different fucosylation levels were subjected to LCA-affinity electrophoresis using an AFP Differentiation Kit L (Wako Pure Chemicals). The procedures are described in detail in the Experimental Section. The bands corresponding to AFP-L1 (nonfucosylated AFP) and -L3 (fucosylated AFP) are indicated by arrows. WT and DKD indicate wild-type cells and cells with a double knock-down of GMD and FX, respectively. Each column represents the mean plus SD for three different experiments. *, significantly different ($p < 0.05$) from wild type; ##, significantly different ($p < 0.01$) from without fucose.

glycoproteins into bile. Fucosylated AFP might exhibit higher affinity for this receptor and might be given priority for secretion into bile, compared with other glycoproteins such as AGP. Therefore, fucosylated AFP, exhibiting higher affinity for the receptor, might not be secreted into serum in the liver with chronic liver diseases, whereas fucosylated AGP, exhibiting lower affinity, is secreted into serum. Comunale et al. reported that increases in alpha1−6 fucosylation on alpha1-antitrypsin were HCC-specific, while increased outer arm fucosylation was observed in both cirrhosis and HCC patients.[28] This report supports our hypothesis that glycoproteins that possess alpha1−6 fucosylated oligosaccharides, including fucosylated AFP, are more selectively secreted into bile. On the other hand, as shown in Figure 3, a percentage of peak 7 material, alpha1−6 fucosylated biantennary structure, in the conditioned medium was significantly higher than that in the BC structures. These data do not seem to be consistent with our hypothesis that alpha1−6 fucosylated glycoproteins are selectively secreted into